공학석사 학위논문

Blue fluorescent Organic Light-Emitting Diodes using exciplex host

엑시플렉스 호스트와 형광 염료를 이용한

청색 형광 유기발광다이오드

2020 년 2 월

서울대학교 대학원

재료공학부

함 진 현

Blue fluorescent Organic Light-Emitting Diodes using exciplex host

지도 교수 김 장 주

이 논문을 공학석사 학위논문으로 제출함

2020 년 1 월

서울대학교 대학원

재료공학부

함 진 현

함진현의 공학석사 학위논문을 인준함

2020 년 1 월

위 원 장 박 수 영 (인)

부위원장 김 장 주 (인)

위 원 장 지 영 (인)

Abstract

Blue fluorescent Organic Light-Emitting Diodes using exciplex host

Jin-Hyun Ham

Department of Materials Science and Engineering

The Graduate School

Seoul National University

A display is a comprehensive word of an imaging device that converts an output signal of an electronic device into visual information and displays it on a screen. The display industry has been continuously developed from liquid crystal displays (LCD), light-emitting diodes

(LEDs), organic light-emitting diodes (OLEDs) to micro and large-area displays, and is being actively researched.

OLEDs expressed as a self-luminous display that uses organic materials to express color and light without a backlight. The fundamental working principles of OLEDs are described below. When an external voltage source is applied to the device, charge carriers are injected; When free holes and electrons recombine each other, they form excitons to emit photons.

OLEDs have many advantages such as no need for backlight or color filters which can reduce volume, provide low power consumption, fast response speed, excellent contrast ratio, wide viewing angle, and the possibility of expansion into a transparent or flexible, foldable display. Because of these advantages, OLEDs are noted as next-generation displays. However, still several challenges need to overcome for better applications in OLEDs industry.

In order to achieve high color purity, high efficiency, and long device operating lifetime in organic light-emitting diodes, research has been ongoing. Since the color is determined by the intrinsic properties of the emitter, proper selection of materials is the most important in OLEDs.

For selecting emitter, various materials such as single molecules, heterogeneous molecules, exciplexes, fluorescent dyes, phosphorescent dyes, and thermally active delayed fluorescent (TADF) materials can be used and various color emission also possible because of multiple choice possibilities of emitters. Among the various colors of OLEDs, the case of blue OLEDs, exciplex forming materials have to satisfy energy levels larger than 2.8 eV. (E_A^{LUMO}-E_D^{HOMO}-E_b) It is difficult to select a common host forming an exciplex with high triplet energy and blue emission, and it has been a problem in terms of stability because a high driving voltage is required when driving the device. That's why blue OLEDs exhibit lower efficiency and device stability compared to devices showing other color emission. Therefore, blue OLEDs have been continuously studied as hot issues to be solved for use in daily life or industry.

This thesis is about the research topic of stable conventional fluorescent OLEDs using greenish-blue and blue exciplex co-hosts.

In **Chapter 2**, devices that show greenish-blue light emission based on exciplex with high $k_{ISC} \times k_{RISC}$ is introduced. Due to the high thermal stability (T_g) of constituent materials, high stability was expected while forming exciplex.[79] Using the combination of molecules which

contain spiro-annulated structure hole transporting material (HTM) with phosphine oxide containing high triplet energy (T_1) electron transporting material (ETM), novel exciplex forming co-host was designed with the peak energy of 2.54 eV. Also, greenish-blue exciplex formed by [8,8′-spirobi[indolo(3,2,1-de)acridine] (H2)] and [(1,3,5-triazine-2,4,6-triyl)tris(benzene-3,1-diyl)]tris(diphenylphosphine oxide) (PO-T2T)] shows high (k_p, $k_{ISC} \times k_{RISC}$) kinetic constants which enable efficient triplet harvesting and collect radiative excitons. Based on new exciplex systems, fabricated OLED achieved 10.6% of maximum EQE.

Operational device stability is one of the areas to be addressed in OLEDs. In **Chapter 3**, to apply exciplex forming co-host based OLEDs, I used yellow conventional fluorescent dopant for fabricating fluorescent OLEDs with extended operational device lifetime using an exciplex co-host. According to the photophysical properties, I found that the energy transfer process to yellow fluorescent emitter can occur well because of spectra overlap between absorption of dopant and photoluminescence (PL) of exciplex. Utilizing a new exciplex system with a yellow fluorescent dopant, the fluorescent OLEDs achieved 7.2% maximum EQE. This device showed an operational lifetime (LT_{50}) over 60hours at 1000 cd m^{-2}.

In the last few decades, designing materials and optimization of device structure have been executed for better efficiency and stability of OLEDs. However, still, it is challenging in blue OLEDs part because it is hard to find out suitable materials for blue exciplex which have to satisfy energy levels larger than 2.8 eV. (E_A^{LUMO}-E_D^{HOMO}-E_b) In **Chapter 4**, novel deep blue exciplex and exciplex-based blue fluorescent OLEDs were introduced. The color gamut Commission Internationale de L′ Eclairage (CIE) of exciplex OLEDs (CIE y < 0.13) was shown in a deep blue region. Expanding the basic concept of fabricating fluorescent OLEDs, I used blue fluorescent emitters to keep pure blue color emission. As a result, a blue fluorescent OLEDs with a maximum EQE of 5.22%, 4.81% was achieved.

Keywords: Fluorescent organic light-emitting diodes, exciplex, maximum EQE, conventional fluorescent emitter, efficient triplet harvesting, energy transfer

Student Number: 2018 – 27446

Contents

List of Tables

List of Figures

Chapter 1. Introduction

1.1 Brief introduction of organic light-emitting diodes

Organic light-emitting diodes (OLEDs) are devices, based on the use of organic molecules to conduct large amounts of charge, which recombines to emit light. Normally, the structure of OLEDs consists of Anode / organic transporting materials / Cathode. Furthermore, organic transporting materials are divided into three-layer: hole transporting material (HTM) / emitting layer (EML) / electron transporting material (ETL). (Figure 1.1)

The fundamental working principles of OLEDs are described below. When an external voltage source is applied to the device, charge carriers are injected; holes from anode and electrons from cathode then moves to the transporting layer. When free holes and electrons recombine each other, they form excitons in the emissive layer (EML) leading to emit photons.

OLEDs are addressed in the new field of flat-panel display due to their various advantages in the wide fields. In recent years, OLEDs attract huge attention for a large area, low cost and also can apply in

lightweight, ultra-thin and flexible electronics. Since there are many advantages and wide field of application are expected, active researches are underway after the 20th century. In 1987, C. Tang and S. A. VanSlyke.[1] proposed a multi-layer structure of thin-film and 1% external quantum efficiency (EQE) electroluminescent (EL) devices under vacuum deposition with below structure; indium tin oxide (ITO) / 1,1-Bis[(di-4- tolylamino)phenyl]cyclohexane (TAPC) / tris(8-hydroxyquinolinato)aluminum (Alq_3) / Mg:Ag. Since this discovery, OLEDs have been actively researched and evoked scientific curiosity to a commercial applications incorporated into devices for bright displays that showing vivid colors and challenges to longevity until nowadays. Figure 1.2 shows the commercial products and applications adopting OLEDs such as a mobile phone, signature television with a large area, OLED wallpapers with multiple display and back light of automobiles.

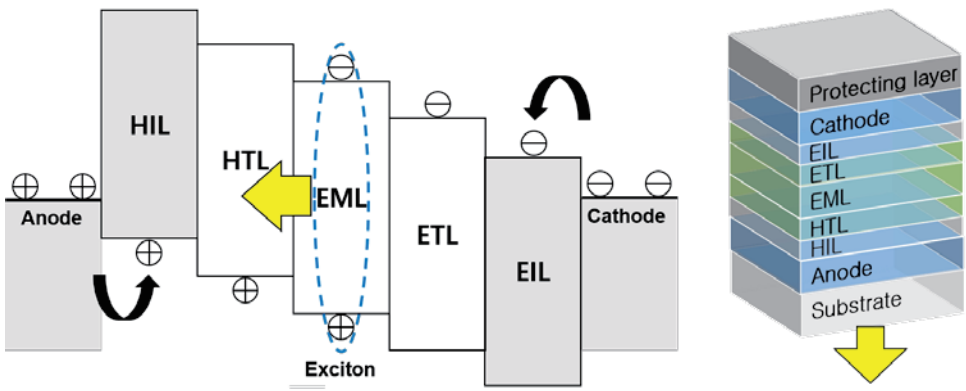

Figure 1.1 Schematic diagram of charge generation mechanisms in organic light-emitting diodes (OLEDs)

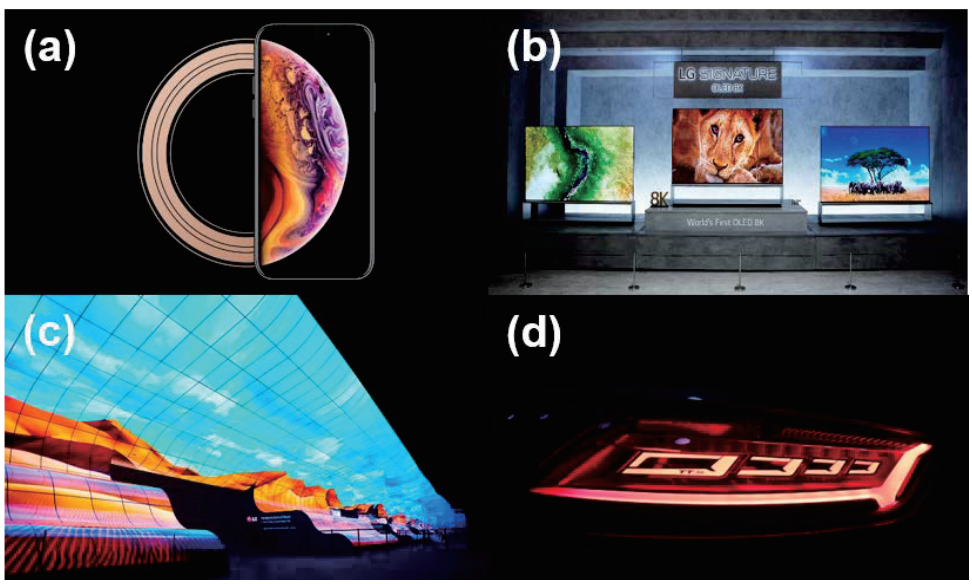

Figure 1.2 Commercial products and applications adopting OLEDs. (a) Apple iPhone 11 Pro applying curved OLED panel (Apple 2019) (b) LG signature TV (LG display 2019). (c) LG OLED Falls (LG Electronics 2019). (d) OLED lighting in automobile (Audi 2016).

1.2 Determining factors in efficiency of OLEDs

In OLEDs, EQE is the representative parameter for the efficiency. EQE is defined as the ratio between the number of emitted photons per injected charge carriers in OLEDs. (Equation 1.1)[2]

$$\eta_{EQE} = \eta_{int} \times \eta_{out} = \gamma \times \eta_{S/T} \times q_{eff}(\phi_{PL}, \Gamma) \times \eta_{out}(\Theta, \Gamma) \qquad (1.1)$$

Basically, the external quantum efficiency (η_{EQE}) can be expressed as multiply of internal quantum efficiency (η_{int}) and out-coupling efficiency (η_{out}). In detail, γ is the charge carrier balance factor, accounting for the same amounts of charge carriers are injected and an equal portion of them recombines to form an exciton. $\eta_{S/T}$ is the singlet-triplet factor which also considered as components affecting η_{int} of OLEDs. In terms of spin-statistics, in the case of two electrons, the singlet has a spin in the opposite direction and the case of spins in the same direction are called triplets. The ratio of singlet to triplet is 1:3, which means that the singlet 25% triplet 75% is generated. Fluorescent emitters can assume $\eta_{S/T}$ as 0.25 and for the phosphorescent emitters as 1. $q_{eff}(\phi_{PL}, \Gamma)$ is the effective radiative quantum efficiency factor,

which depends on photoluminescence quantum yield (PLQY) and the geometric factor (Γ). $q_{\text{eff}}(\phi_{\text{PL}})$ is expressed as below. (Equation 1.2)

$$q_{\text{eff}}(\phi_{\text{PL}}) = \frac{k_{\text{r}}}{k_{\text{r}} + k_{\text{nr}}} \tag{1.2}$$

k_{r} and k_{nr} represent of radiative decay rate and non-radiative decay rate each. In cavity structure, different indices of refraction inherent in different materials will affect the radiative decay rate of the exciton, which also takes into account as Purcell factor.[21,22,23] However, in the non-radiative decay rate, are not affected by the cavity structure so we don't need to consider Purcell factor.[24] $\eta_{\text{out}}(\Theta,\Gamma)$ is the out-coupling efficiency factor, which depends on the horizontal ratio of an emitting dipole (Θ) and the geometric factor (Γ). These are related to the orientation of emitter which contributed to the degree of light extraction.[25,26,27] Many studies have been conducted on OLEDs using molecules having a high horizontal orientation ratio, which showed high EQE.[2-3,28,29-39]

1.3 Exciplex-based OLEDs

Exciplex stands for excited-state charge transfer complex. It is formed between donor and acceptor molecules while they are excited. Basically, the highest occupied molecular orbital (HOMO) and lowest unoccupied molecular orbital (LUMO) energy levels of the donor molecule are higher than acceptor molecule. Since exciplex formation can occurr as the charge transfer (CT) from a locally excited (LE) molecule to counterpart one, the wave function of the exciplex can be expressed as a combination of LE, CT, and neutral ground states.[42,43]

Exciplex in solid-state is assumed to have various geometric difference and distances between donor and acceptor molecules. Thus, Photoluminescence (PL) spectrum of exciplex normally shows broad, featureless, and red-shifted emission from the constituting materials (donor, acceptor molecule) emission.[44] Also exciplexes are expected to have small ΔE_{ST} which enables efficient reverse intersystem crossing (RISC) process due to the lower overlap between the frontier orbitals.[45,46,47]

In the twentieth century, the formation of exciplex was thought of as the reducing factor in the efficiency of OLEDs.[48,49,50] However, this

perception changed after few advantages of exciplex were reported. Exciplexes have small ΔE_{ST} which enables efficient intersystem crossing (ISC) and reverse intersystem crossing (RISC) process for additional efficiency. There are two ways of fluorescence. One is molecules in the singlet state can fluorescence to ground state rapidly called prompt fluorescence (PF) and another is delayed fluorescence (DF) that fluorescence after singlet state being back from the ISC and RISC cycles. Exciplex utilizes both PF and DF for efficient triplet harvesting.

A number of papers have been published with exciplex forming co-host as the emitter in OLEDs.[19,45-47,51-60] Also, exciplex-sensitized conventional fluorescent[4,41,67-70] and phosphorescent OLEDs have been reported.[2-5,8,29,61-66]

1.4 Generation of OLEDs

A large number of OLEDs papers have been published since C. Tang and S. A. VanSlyke reported a representative EL device in 1987, to date that OLEDs are divided into three generations.[1,4,5-20] The first generation OLEDs were based on fluorescent emitters that only the singlet excited states can participate in light emission while triplet states dominantly emit heat.[4,41,67-70] When emitting light, fluorescence has a different spin direction (singlets), so it emits light quickly and easily when electrons fall to the ground.

Second generation OLEDs were based on phosphorescence emitters with heavy metal complexes are called phosphorescent OLEDs.[2-5,8,29,61-66] In this case, triplet excited states can be fully utilized for light emission and also singlet excited states which enable an internal quantum efficiency of up to 100%. Phosphorescent emitter (organo-metallic compound) containing heavy metal atoms are capable of transition between different spin states because of spin-orbit coupling (heavy-atom effect).[5] When emitting light, due to phosphorescence has the same spin direction (triplets), the electrons are slow to fall to the ground state, the light is emitted slowly and the emission time is long.

Third generation OLEDs were based on thermally activated delayed fluorescence (TADF) emitters and triplet-triplet annihilation (TTA) process.[16,17,18-20] The big difference between TADF and TTA is the number of molecules that involved in reaction; TADF is a reaction of a molecule and TTA is a reaction of biomolecules.[18,19,20] H. Uoyama et al., developed TADF materials which shown small singlet and triplet excited states gap (ΔE_{ST}), to harvest triplet excited states without heavy metal.[6] Donor-acceptor structures have been widely used in TADF emitters for intra-, inter-molecular energy transfer and to convert the triplet state excitons to the singlet state via a reverse intersystem crossing. Second generation OLEDs (Phosphorescence) and third-generation OLEDs (TADF) were based on the spin mixing process of singlet and triplet excited states. However, the lifetime of OLEDs still needs to progress because of the long decay time caused by the spin-mixing process.

To solve the slow decay process in the emitters, research has been carried out to harvest triplets using conventional fluorescence dyes as emitters.[9,10,12-15] Sensitizing is one of the methods using a spin-mixing mediator, so-called sensitizer while designing emitting material. Organo-metallic compounds or TADF materials or Exciplex has been studied as

a suitable sensitizer. M. Baldo et al. firstly reported fluorescent OLEDs using a phosphorescent sensitizer.[9] They used 4,4′-*N,N*′-dicarbazole-biphenyl (CBP) as the donor and host material, tris(2-phenylpyridine) iridium ($Ir(ppy)_3$) as sensitizer, 4-(Dicyanomethylene)-2-methyl-6-julolidyl-9-enyl-4H-pyran (DCM2) as a fluorescent dye. While excitons are transferred to the singlet state of the fluorescent dye, an additional spin-mixing process caused by heavy metal complex inducing more probability of energy transfer into the singlet state of the fluorescent dye and also by a Förster energy transfer process.

H. Nakanotami et al. reported fluorescent OLEDs using a TADF sensitizer in 2014.[10] Up-conversion from triplet states to the singlet state of the TADF molecule, and these additional up-converted singlet state can be transferred to singlet excited state of the fluorescent dye via a Förster energy transfer process.

The second method for overcame theoretical limit of 25% in fluorescent is called extra-fluorescence. M. Segal et al. reported fluorescent OLEDs using a mixed layer inserted structure which affects charge transfer (CT) states that act as precursors to excitons.[15] They used Alq_3 doped with PtOEP as the emissive layer (EML). This system shows that the CT spin mixing process can enormously increase the fraction of

singlet excitons in fluorescent materials because of the CT spin mixing process caused by heavy metal in organo-metallic compounds.

Based on the two methods written above, these results clearly showed that the fluorescent OLEDs overcame the theoretical limit for the singlet exciton formation efficiency.

Recently, Adachi et al. reported almost 30 to 40% EQE from phosphorescence-based OLEDs with thick MAPbCl3 transport layer and light-scattering sheet.[40]

Through the various generation of OLEDs, still have more possibility and needs more challenge for a novel strategy to improve the efficiency and operational stability of OLEDs. As with these, OLEDs should develop more and more. Overall schematic diagram of the excited-state process; so-called various generation of OLEDs are illustrated in figure 1.3 and figure 1.4

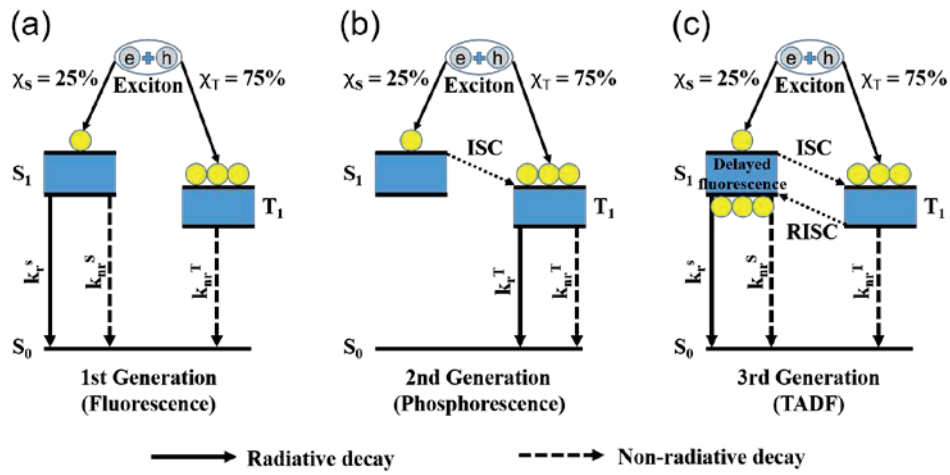

Figure 1.3 Schematic diagram of excited-state process; (a) 1st generation: Fluorescent OLEDs (b) 2nd generation: Phosphorescence OLEDs (Organo-metallic compounds) (c) 3rd generation: Thermally activated delayed fluorescence (TADF) OLEDs.

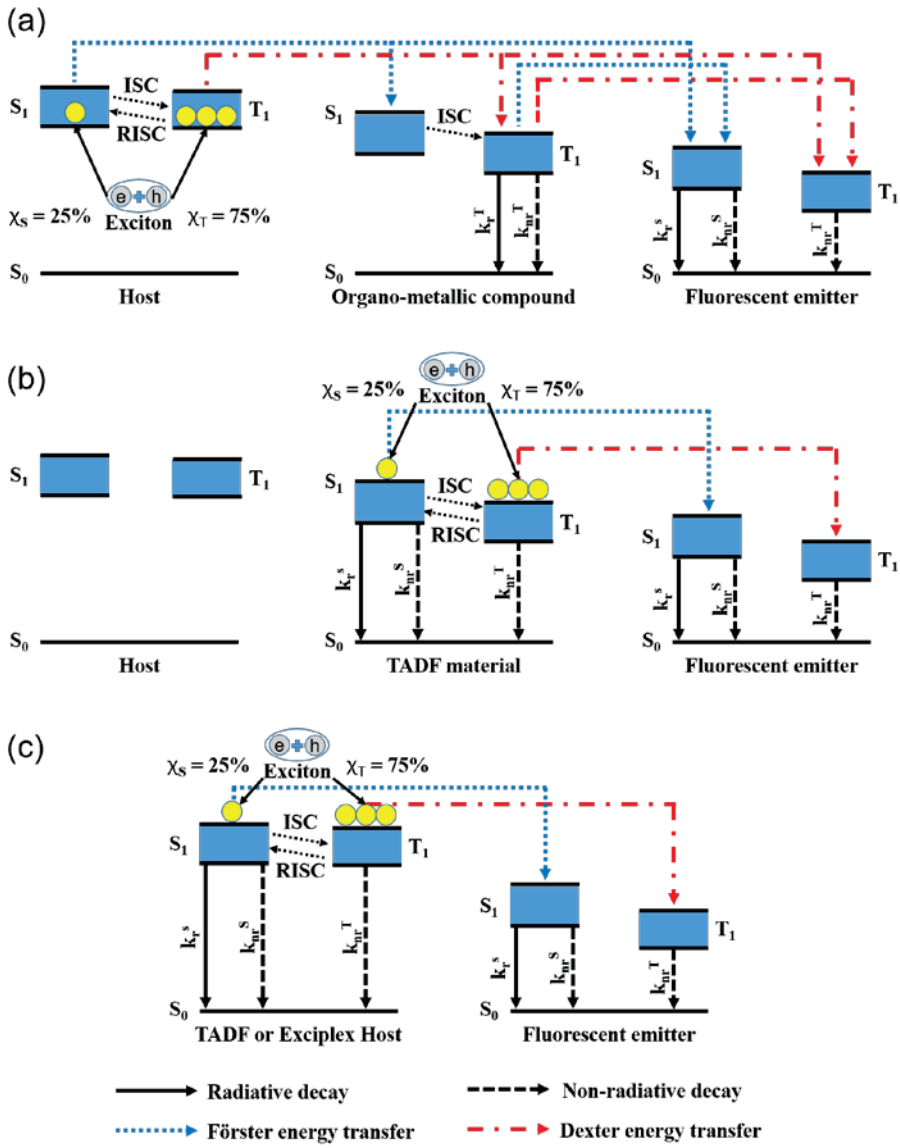

Figure 1.4 Schematic diagram of excited-state and energy transfer process in fluorescent OLEDs (a) Phosphorescent-sensitized OLEDs (b) TADF-sensitized OLEDs (c) Fluorescent OLEDs based on TADF or exciplex host.

1.5 Outline of thesis

In this thesis, generally introduces a novel exciplex system and its expansion to conventional fluorescent OLEDs based on exciplex forming co-hosts. Especially addressed on the blue emission because of the low efficiency and instability of blue fluorescent is an issue to the commercialization of OLEDs, which need to be solved.

New exciplex forming co-host for greenish-blue emission has been developed. Exciplex system consists of thermally stable molecules as donor and acceptor. Using this exciplex system, a device with 10.6% of maximum external quantum efficiency (EQE) was achieved. Also, observation of EL spectra red-shift caused by voltage increment in greenish-blue exciplex OLEDs analyzed as to its own unique characteristic (Chapter 2).

Based on the novel greenish-blue exciplex system reported in Chapter 2, I designed conventional fluorescent OLEDs based on exciplex forming co-host and yellow fluorescent emitter. I tried to fix the EL spectra of the H2:PO-T2T exciplex system in which the EL spectra changes with applied voltage. Also, greenish-blue H2:PO-T2T exciplex system has a high delayed components ratio (k_{ISC}·k_{RISC}, Φ_d), which

speculated as triplet harvesting would increase the proportion of singlet excitons that could emit additional light if energy transfer occurs well from exciplex to a conventional fluorescent emitter. The yellow fluorescent OLED showed a 7.2% maximum EQE. Besides, the operational device lifetime of fluorescent OLED was measured as 60 hours, which is 8.5 times longer than TCTA:B4PYMPM exciplex co-host based fluorescent OLEDs with the same fluorescent emitter and doping condition. Confirmation of energy transfer occurs well in this exciplex system and also energy transfer process reduces the excited-state excitons lifetime of the exciplex in fluorescent material, resulting in improvement of the device operational stability of the OLEDs (Chapter 3).

Various emission range exciplex forming co-host based OLEDs with fluorescent dopant system has the potential to reach operational stability and efficiency with better color purity for fluorescent OLEDs. However, the exciplex forming co-host for deep-blue fluorescent OLEDs has been rarely reported because it is hard to find out suitable materials forming exciplex not only for blue emission range but also for transporting energy gap of exciplex should be larger than 3.0 eV or optical bandgap larger than 2.7 ~ 2.8 eV. I designed a new deep-blue

exciplex system using hole transporting material (HTM) with carbazole moieties and electron transporting material (ETM) with triphenyl-phosphine oxide moieties. Based on the exciplex system, a fluorescent device was fabricated using the blue fluorescent emitters. Fabricated blue fluorescent OLEDs showed a maximum EQE of 5.22%, 4.81% and an operational lifetime (LT_{50}) of 0.4, 2.7 hours. Also fluorescent OLEDs showed EL peak wavelength (λ_{max}^{EL} : 464nm / 464nm) and color coordinate (CIE *x*, CIE *y*: 0.13, 0.22 / 0.13, 0.17) indicating these results are well-matched with blue emission. (Chapter 4).

Chapter 2. Greenish-blue exciplex forming co-host based Organic Light-Emitting Diodes with 10.6% External Quantum Efficiency and high $k_{ISC} \cdot k_{RISC}$ rate constants

2.1 Introduction

Excited-state charge-transfer complex (Exciplex) was used as one of the candidates for composing the emitting layer. Exciplex forming co-hosts have outstanding advantages in OLEDs history, for example, exciplex forming co-host systems are expected to have small ΔE_{ST} which enables efficient reverse intersystem crossing (RISC) process due to the lower overlap between the frontier orbitals.[45,46,47] Up to now the efficiency of exciplex which is used as the emitter in OLEDs, has been reported showing EQEs of 5~20% without dopant.[19,45-47,51-60]

Recently, the maximum external quantum efficiency (EQE) up to 20% of exciplex-based OLEDs has been achieved by using a triplet-confined exciplex system with 100% photoluminescent quantum yield (PLQY).[57] In triplet-confined exciplex system, where triplet energy is

bound to the exciplex, that reverse energy transfer from the exciplex to the electron donor or acceptor seems prohibited. And this can be one of the factors that influences on PLQY.[77]

In this chapter, bulky and diagonal configuration core structure, a spiro-bonded molecule based on indolo-acridine (H2) was selected as a donor and having phosphine oxide moieties based on triazine core structure (PO-T2T) was used as an acceptor. It was intended to design an exciplex system that satisfies the triplet-confinement using molecules with high triplet energy larger than 2.90eV. [61,76,78] The spiro-bond main core structure worked as donor providing high triplet energy over 2.90 eV and the acceptor with a phosphine oxide also providing high triplet energy over 2.99 eV. Also expected that composing exciplex with a thermally stable donor can form stable exciplex for better PLQY which influences on EQE.

This work presents highly efficient ($k_{ISC} \times k_{RISC}$) kinetic constant based on a new exciplex-forming co-host consisting of a hole-transporting material [8,8′-spirobi[indolo(3,2,1-de)acridine] (H2)] and an electron-transporting material containing phosphine oxide moieties based on triazine-core structure [(1,3,5-triazine-2,4,6-triyl)tris(benzene-3,1-diyl)]tris(diphenylphosphine oxide) (PO-T2T)]. The H2:PO-T2T

exciplex forming co-host based OLED shown a maximum EQE of 10.6% and a current efficiency (CE) of 24.4 cd A^{-1} with low operating voltage 2.7 V. More interestingly, the device using the H2:PO-T2T exciplex shows EL spectra red-shift while applying voltage and this situation was reversible.

2.2 Experimental

2.2.1 Organic film fabrication

To fabricate organic film samples, cleanly washed quartz substrates should be prepared after the piranha treatment. The way to dissolve the solution for the piranha treatment is to mix sulfuric acid (H_2SO_4) and hydrogen peroxide (H_2O_2) in a 3:1 ratio. The piranha process is done by dipping the substrate in the piranha solution for at least 1hour and 30 minutes and rinsing with deionized water. After piranha treatment, all substrates were cleaned using isopropyl alcohol and acetone inside of a bath to remove remains. The organic layers were deposited on a quartz substrate by thermal vacuum-evaporation under a pressure of 5.9×10^{-8} Torr. Metal masks were used to form an active area of 2×2 mm^2 and to fabricate various conditions. In a single material layer was deposited at a rate of 1 Å/s and the deposition rate of the co-deposited layers was 1 Å/s in total, which was calculated in proportion to the molar mass of composing materials.

2.2.2 Device fabrication

To fabricate exciplex OLEDs, the organic layers and aluminum (used as an electrode) were deposited on top of 70-nm-thick indium tin oxide (ITO) by the thermal vacuum-evaporation process under a pressure of $< 1\times10^{-7}$ Torr. Metal masks were used to form an active area of 2×2 mm^2 and to fabricate various conditions. Before deposition, all 70-nm-thick ITO substrates were pre-heated at 250 ℃ for 30 minutes and rinsed with deionized water. After the rinsing process, all substrates were pre-cleaned using isopropyl alcohol and acetone inside of a bath to remove remains. Next, the substrates were exposed under a UV-ozone flux for an overall 6 minutes. (1 minute 30 seconds for nitrogen, oxygen each and 3 minutes for UV light) In a single material layer was deposited at a rate of 1 Å/s and the deposition rate of the co-deposited layers was 1 Å/s in total, which was calculated in proportion to the molar mass of composing materials. The deposition rate of aluminum (used as an electrode) was 4 Å/s. The fabricated devices were encapsulated with a cover glass using UV-curable resin in a glovebox before the measurement of device properties.

2.2.3 Photophysical properties of an organic film

The Absorption spectra of organic films were measured using Cary 5000 UV-vis-NIR (Agilent Technologies) spectrophotometer. The PL spectra of organic films were measured using a spectrofluorometer (Photon Technology International) connected to a monochromator (Acton Research). The excitation wavelength of xenon-lamp was fixed as 325nm for H2 neat film and H2:PO-T2T mixed film. To measure the solution PL spectra, H2 material was diluted in MC solvent to 10^{-3}, 10^{-4}, 10^{-5} M. The Solution PL spectra of H2 material was measured using a He-Cd laser (325 nm) as the excitation source and a fiber optic spectrometer (Ocean Optics Maya 2000) as the optical detection system. To measure the PL efficiency, organic materials were deposited on quartz substrates in 30-nm thickness. 6-inches diameter integrating sphere (Labsphere Co.), pasted with barium sulfate ($BaSO_4$) was served as a darkroom for measuring accurate efficiency value, and a monochromator (Acton Research Co.) attached to a photomultiplier tube (Hamamatsu Photonics K.K.) was used as the optical detection system. Detailed experimental information for calculation of PL efficiency value is described in previously reported papers.[71,72,73] To measure the transient

PL signals, nitrogen laser (337 nm) was used as the excitation light source, and a streak camera (Hamamatsu Photonics) was used as the optical detection system. Angle-dependent PL (ADPL) experiment was performed using a fiber optic spectrometer (Ocean Optics Maya2000). ADPL measurement behaved on automatically rotating stages and half-cylinder lens. The organic film attached to a half-cylinder lens without any refractive index difference using index matching oil. Detailed experimental information for the experimental setup is described in previously reported papers.[2,34,74-75]

2.2.4 Device characterization

Current density, luminance, and EL spectra were measured using a programmable source meter (Keithley 2400) and a radiometer (SpectraScan PR650). The EQEs and power efficiency of OLEDs were obtained from overall data of current density-voltage-luminance (*J-V-L*) characteristics, EL spectra, and Lambertian correction factors.

2.3 Result and discussion

PLQY is one of several parameters that make up the EQE to evaluate efficiency among device characteristics. Even there are many factors influence photoluminescence quantum yield (PLQY) such as environment, morphology and so on, the basic concept of designing high PLQY of materials without any optical loss channel needs to satisfy triplet-confinement while forming exciplex.[77] Basically, energy transition takes place from high energy to low energy. In the triplet non-confined exciplex system, there is a possibility of an energy leakage pathway between exciplex and constituting molecules because the low energy triplet state of constituting molecules is positioned below exciplex states. Thus, it is important to remind that the high triplet energy levels of materials forming exciplex are a necessary requirement for better efficiency of OLEDs. This basic concept is explained schematically in Figure 2.1.

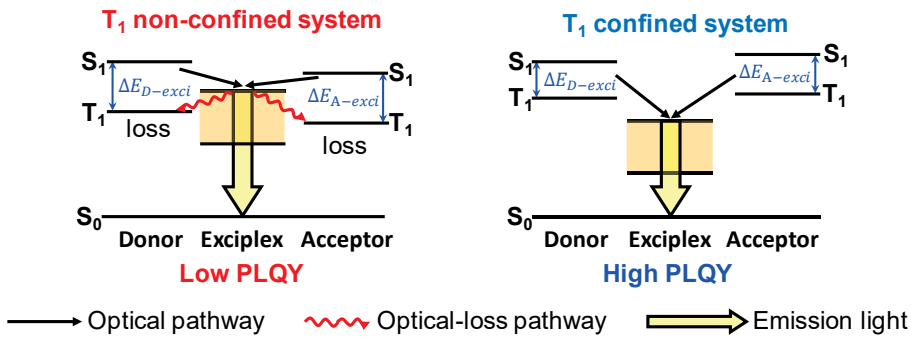

Figure 2.1 Schematic illustration of the correlation between with or without triplet-confined exciplex system and PLQY value.

In this work, we report a novel greenish-blue exciplex OLEDs based on a triplet-confined system with high (k_p, $k_{ISC} \times k_{RISC}$) kinetic constants and more delayed fluorescence components. The OLEDs showed a maximum EQE of 7.5% and a driving voltage of 2.7 V. Furthermore, reducing the formation of interface exciplex, 5 nm neat HTM layer was inserted between HTL and EML. As a result, a greenish-blue device with a 10.6% maximum EQE device was fabricated. And this result showed 1.4times increment in EQE compared with the previous one and almost 63 ~ 72% of radiative singlet excitons (η_s) were related to the emission process harvested through the delayed components.

[8,8′-spirobi[indolo(3,2,1-de)acridine] (H2)] was selected as donor material and [(1,3,5-triazine-2,4,6-triyl)tris(benzene-3,1-diyl)]tris(diphenylphosphine oxide) (PO-T2T)] was selected as acceptor material to form an exciplex. Figure 2.2a and figure 2.2b show the chemical structure of the materials used in the devices, along with the emitting layer structure, the highest occupied molecular orbital (HOMO), lowest unoccupied molecular orbital (LUMO), and triplet energy levels.[61,76,78] H2:PO-T2T (molar ratio of 1:1) co-deposited film was used as the host and this exciplex satisfies triplet confinement.

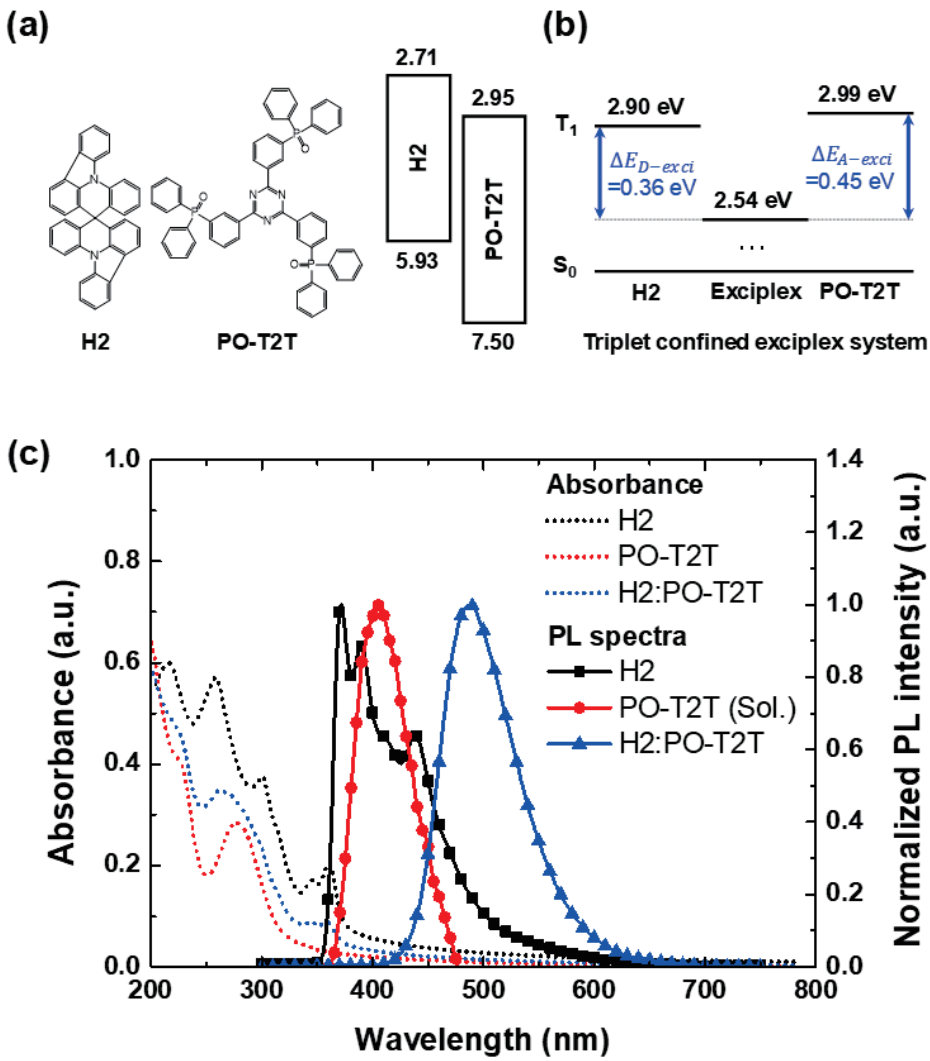

Figure 2.2 (a) Chemical structures and energy levels of H2 and PO-T2T. (b) Triplet energy diagram of host materials (H2, PO-T2T) with H2:PO-T2T exciplex. (c) Room-temperature absorption spectra and PL spectra of H2, PO-T2T, mixed H2:PO-T2T (30 nm-thick thin films)

- Energy levels were determined by CV or UPS.
- LUMO of H2 was calculated by HOMO and the optical gap

Figure 2.2c shows that the mixed film forms exciplex obviously by the appearance of a broad, featureless PL spectra redshifted from those of H2 and PO-T2T.

The transient PL of the H2:PO-T2T exciplex co-deposited film was measured for understanding the kinetic constants. All kinetic constants were extracted as the same method followed by previously reported papers.[46,47,52] Figure 2.3a shows the transient PL data of H2:PO-T2T exciplex integrated from 355 nm to 617 nm and TCTA:B4PYMPM exciplex from 350 nm to 750 nm as reference.[52] The transient PL decays showed delayed emission for all films, indicating that possibility of efficient triplet harvesting occurs in every exciplex system. The rate constants of the prompt emission (k_p) extracted from the steep slope of the decay curves in the nano-seconds scale are about 10 to the power of 7 for H2:PO-T2T exciplex system. (Table 2.1) This value is one order higher than TCTA:B4PYMPM exciplex system[52], which means having a possibility for a better radiative transition portion. Delayed emission constants (k_d) also extracted from low boundary slope of the decay curves in micro-seconds scale, are almost the same as 10 to the power of 4 for overall exciplex systems.

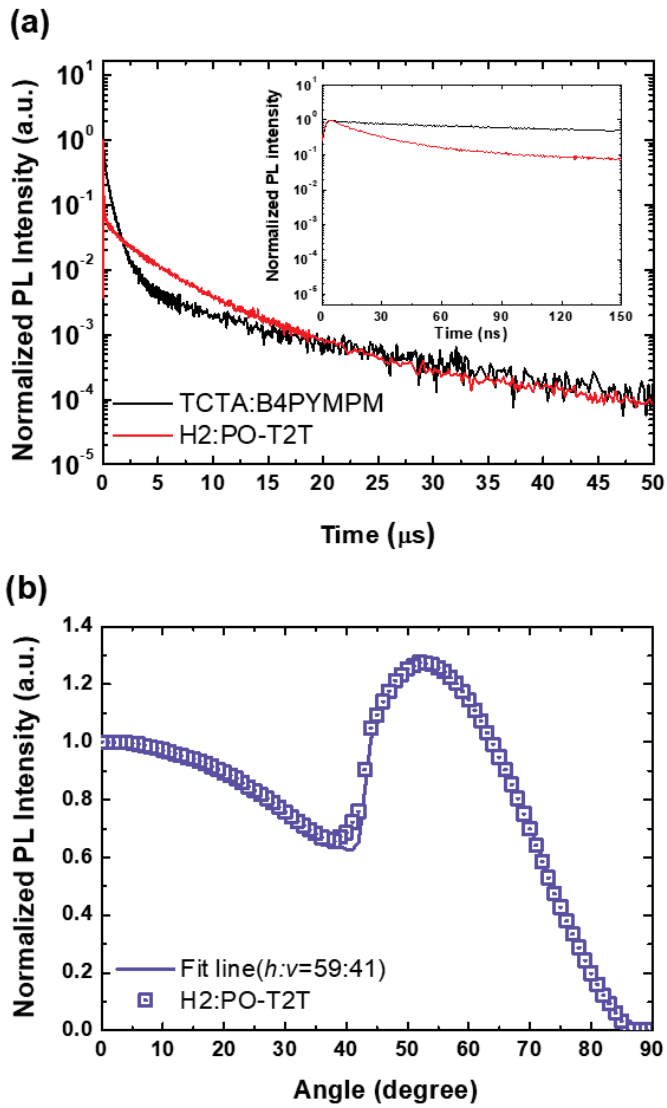

Figure 2.3 (a) Normalized transient PL decay curves of H2:PO-T2T and TCTA:B4PYMPM exciplex film (30-nm-thick deposited on a fused silica substrate) at room temperature. (Inset: prompt decay curves of nanoseconds scale) (b) Experimentally obtained angle-dependent PL intensity of the *p*-polarized light emitted from a 30 nm-thick H2:PO-T2T exciplex film.

Table 2.1 Transition rate constants extracted from transient PL measured data of various exciplex systems at room temperature

	k_p [s^{-1}]	k_d [s^{-1}]	k_r^S [s^{-1}]	$k_{nr}^S+k_{ISC}$ [s^{-1}]	$k_{nr}^T+k_{RISC}$ [s^{-1}]	$k_{ISC}k_{RISC}$ [s^{-2}]	Φ_p [%]	Φ_d [%]	$\Phi_{ISC}\Phi_{RISC}$ [%]
H2:PO-T2T	3.76×10^7	5.67×10^4	3.70×10^6	3.39×10^7	2.93×10^5	8.88×10^{12}	10	41	80
TCTA:B4PYMPM[52]	4.00×10^6	5.26×10^4	1.32×10^6	2.68×10^6	9.60×10^4	1.73×10^{11}	32	28	46

$\tau_{p,d}$: prompt and delayed decay lifetime $k_{p,d}$: prompt and delayed emission decay rate k_{ISC} : intersystem crossing rate
k_{RISC} : reverse intersystem crossing rate $\Phi_{p,d}$: prompt and delayed component of PLQY
k_r^S : radiative transition rate of the singlet $k_{nr}^{S,T}$: non-radiative transition rate of singlet and triplet

However, the delayed kinetic constants ($k_{ISC} \times k_{RISC}$) are one order larger than TCTA:B4PYMPM exciplex system, indicating more delayed cycles can appear in this exciplex system. It was assumed that more delayed portions have a possibility for additional light emission. Overall kinetic constants extracted from the transient PL data of both exciplex systems are summarized in table 2.1.

Kinetic constants of various exciplex systems are extracted from below formulas[46,47,52]:

$$k_{nr}^{s} + k_{ISC} = k_{p} - k_{r}^{s} \tag{2.1}$$

$$k_{nr}^{T} + k_{RISC} = k_{d} + \frac{k_{ISC}k_{RISC}}{k_{p}} \tag{2.2}$$

$$k_{ISC}k_{RISC} = k_{p}k_{d}\frac{\Phi_{d}}{\Phi_{p}} \tag{2.3}$$

$$k_{r}^{s} = k_{p}\Phi_{p} \tag{2.4}$$

$$\Phi_{ISC}\Phi_{RISC} = \frac{\Phi_{d}}{\Phi_{p} + \Phi_{d}} \tag{2.5}$$

The PLQY and emitting dipole orientation were also observed because those are influencing factors in device characteristics such as EQE. The PLQYs of the prompt (Φ_p) and the delayed components (Φ_d) at room temperature was calculated by the integration of the prompt and delayed portion of transient PL data. H2:PO-T2T shows 51% PLQY value.

Figure 2.3b shows that the emitting dipole orientation of H2:PO-T2T exciplex was analyzed using the angle-dependent PL intensity. The angle-dependent PL of H2:PO-T2T exciplex was measured at 487 nm. The experimental data are well fitted by a horizontal-to-vertical dipole ratio of h:v = 0.59:0.41 for H2:PO-T2T indicating that the transition dipole moments of H2:PO-T2T exciplex have a preferred orientation in anisotropic direction.

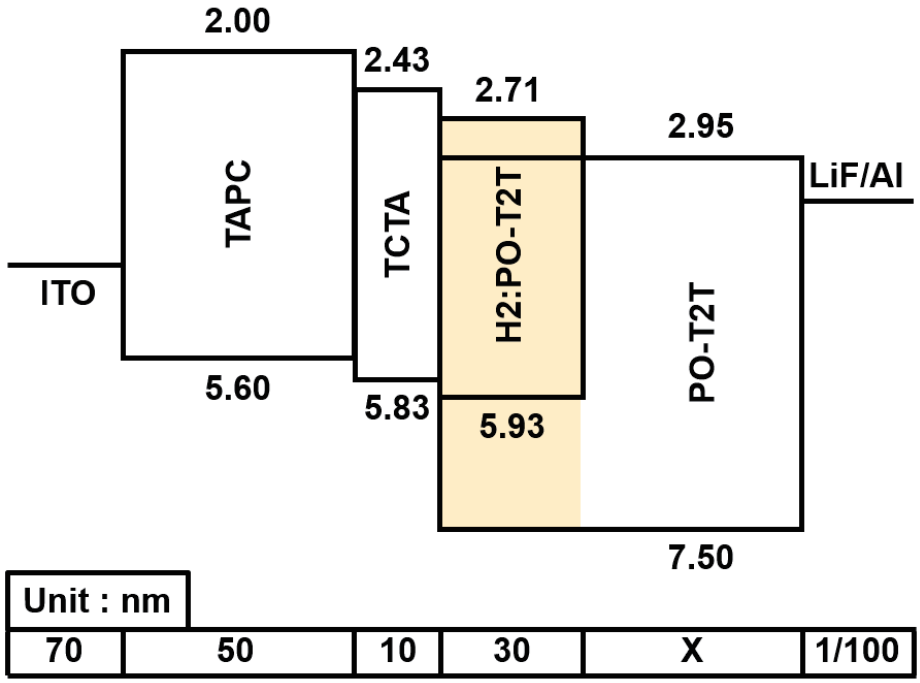

Figure 2.4 Schematic diagram of the device structure and energy levels of the consisting layers of H2:PO-T2T exciplex forming co-host based OLEDs. (Variation of ETL thickness 40nm/50nm/60nm while HTL thickness fixed as 50nm.)

- Every substrate was annealed at 250 ℃ for 30min before evaporation
- ETL thickness variation (30nm/40nm/50nm)
- Energy levels were determined by CV or UPS.
- HOMO levels of TAPC, TCTA and H2: CV measurement
- LUMO levels of TAPC, TCTA and H2: HOMO levels + the optical gap
- HOMO levels of PO-T2T: UPS measurement
- LUMO levels of PO-T2T: CV measurement

An OLED was fabricated based on an exciplex forming co-host as an emitter. The schematic diagram of the device structure and the energy levels of the consisting layers are shown in Figure 2.4. The device structure of OLED is same as follows; ITO (70 nm) / TAPC (50 nm) / TCTA (10 nm) / H2:PO-T2T (30 nm) / PO-T2T (x nm) / LiF (1 nm) / Al (100 nm). The thickness of the electron transporting layer (ETL) was changed from 40 nm to 60 nm at an interval of 10 nm. The current density-voltage-luminance (*J-V-L*) characteristics of the exciplex OLEDs at room temperature with various ETL thickness are shown in Figure 2.5a. It shows the turn-on voltage of 2.7 V to 3.3 V due to different ETL thickness and bandgap. The EQEs and luminance of the devices are displayed in Figure 2.5b. The maximum efficiency of the H2:PO-T2T exciplex forming co-host based OLED was 7.5% with greenish-blue emission. Detailed characteristics of devices are summarized in table 2.2.

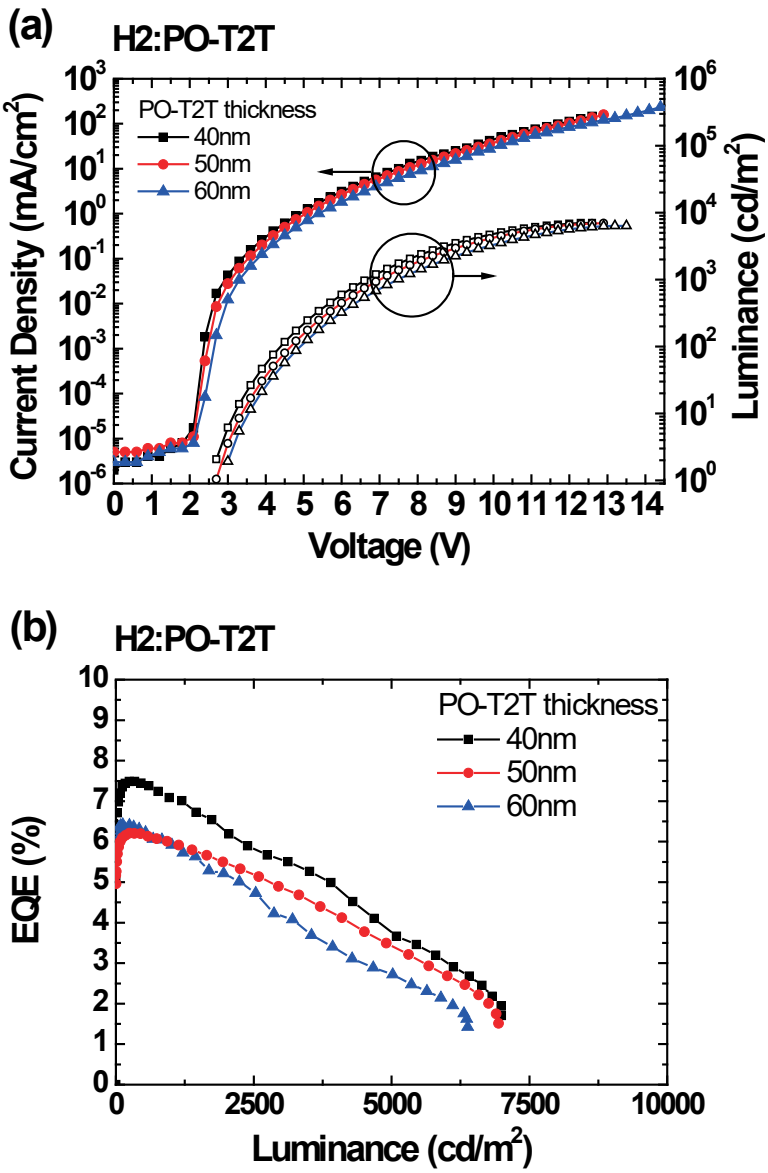

Figure 2.5 (a) Current density-voltage-luminance (*J-V-L*) characteristics of H2:PO-T2T exciplex forming co-host based OLEDs (b) External quantum efficiencies (EQEs) versus luminance curves of H2:PO-T2T exciplex forming co-host based OLEDs

Table 2.2 Device performance of exciplex forming co-host based OLEDs

Device	Voltage [V]		EQE [%]		Current efficiency [cd A^{-1}]		Power efficiency [lm W^{-1}]	
	Turn-on	1,000 cd m^{-2}	Max.	1,000 cd m^{-2}	Max.	1,000 cd m^{-2}	Max.	1,000 cd m^{-2}
H2:PO-T2T	2.7/2.7/3.0	6.9/7.2/7.5	7.5/6.2/6.4	7.0/5.9/5.9	19.4/16.8/17.7	18.5/16.2/16.6	15.2/14.1/16.2	8.4/7.1/6.9

* Variation of ETL thickness **(40nm/50nm/60nm)** while HTL thickness fixed as 50nm.

The EL spectra of fabricated OLEDs are shown in figure 2.6a. Interestingly, EL spectra of H2:PO-T2T exicplex forming co-host based OLEDs shows a red-shifted profile while applying voltage increment. To analyze this phenomenon, firstly I considered the possibility that the location of the emission zone changed from the center of EML to EML located close to HTM or surface of HTM. To confirm this assumption, the simulation was performed using Luxol software, which allows the fabrication of virtual devices and the extraction of device properties. The simulated EL spectra profile (square-dot-plot) and experimentally achieved EL spectra data (line-plot) are shown in figure 2.6b. However, the change of EL peak with the change of emission zone showed a change of about 10 nm from 486 nm to 496 nm, while the experimentally obtained EL spectra showed almost 36nm shift from 496nm to 532nm. Also, full-width at half maximum (FWHM) value was increased from 88nm to 111nm. These results indicate that the location of the emission zone could be one of the factors affecting EL spectra changing profile, but still need progress to understand other factors.

Secondly, I fabricated additional interface-exciplex OLEDs and bulk-exciplex OLEDs to determine whether these phenomena are reversible or due to the inherent property of the H2:PO-T2T exciplex.

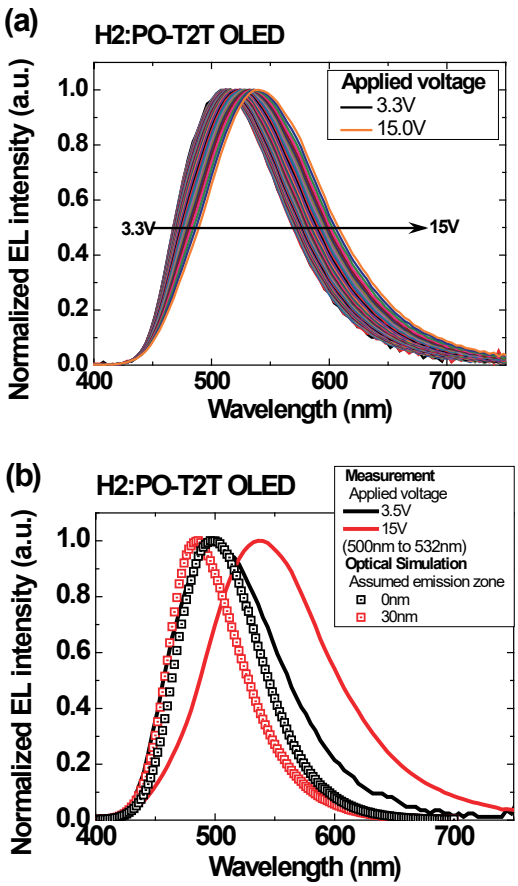

Figure 2.6 (a) Electroluminescence (EL) spectra profile of H2:PO-T2T exciplex forming co-host based OLEDs while applying voltage increment. (b) Comparison of simulation and experimental results for EL spectra shifted profile.

Figure 2.7a and figure 2.7b depict the device structure with its energy levels. The interface-exciplex OLED structure is as followed: ITO (70 nm) / TAPC (50 nm) / TCTA (10 nm) / H2 (30 nm) / PO-T2T (x nm) / LiF (1 nm) / Al (100 nm). In order to observe the profile of the EL spectra at the interface exciplex between pure H2 and PO-T2T, I designed the OLED structure without a mixed co-host.

The bulk-exciplex OLED structure is as followed: ITO (70 nm)/ TAPC (50 nm) / TCTA (10 nm) / H2 (5 nm) / H2:PO-T2T (30 nm) / PO-T2T (x nm) / LiF (1 nm) / Al (100 nm). In order to minimize the possibility of exciplex formation at the interface with TCTA by shifting the emission zone toward HTM, OLEDs having a structure in which a 5nm pure H2 layer is inserted between HTM and EML. The thickness of the electron transporting layer (ETL) was changed from 30 nm to 50 nm at an interval of 10 nm for both OLEDs. Figure 2.8a and figure 2.8b show the current density-voltage-luminance (*J-V-L*) characteristics of the devices. It shows the turn-on voltage of 2.7V to 3.3V due to different ETL thickness and bandgap. The EQEs and luminance of the devices are displayed in Figure 2.8c and Figure 2.8d. The maximum efficiency of the H2:PO-T2T bulk-exciplex OLEDs and interface-exciplex OLEDs were 10.6%, 1.6% each with greenish-blue emission.

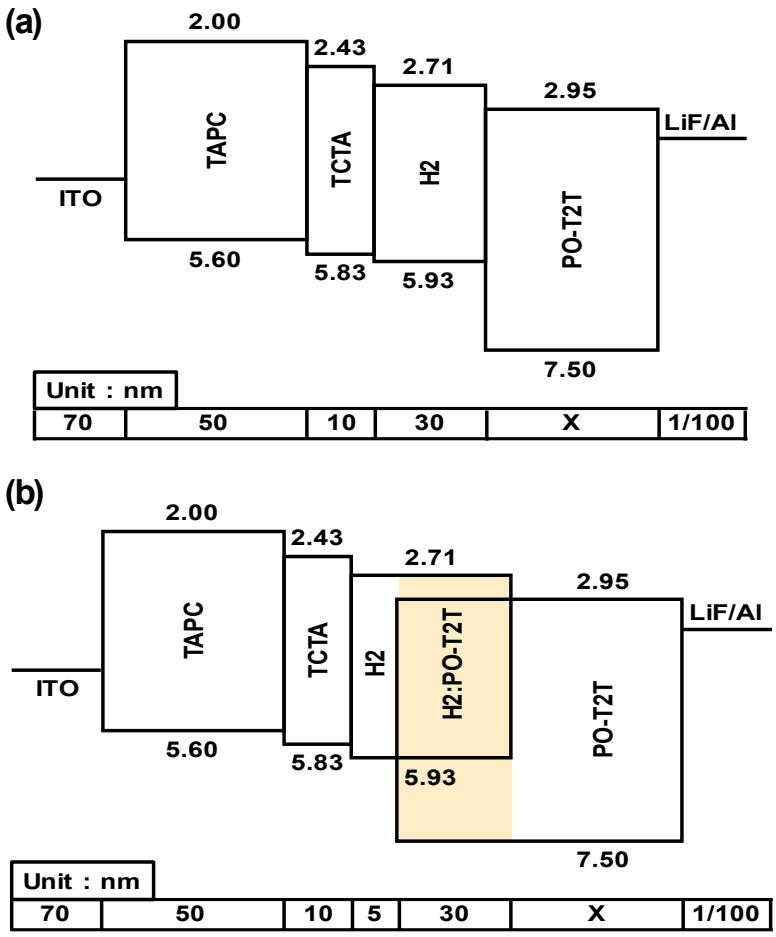

Figure 2.7 (a) Schematic diagram of the device structure and energy levels of the consisting layers of H2:PO-T2T interface-exciplex OLEDs and (b) H2:PO-T2T bulk-exciplex OLEDs.

- Every substrate was annealed at 250 ℃ for 30min before evaporation
- ETL thickness variation (30nm/40nm/50nm)
- Energy levels were determined by CV or UPS.
- HOMO levels of TAPC, TCTA and H2: CV measurement
- LUMO levels of TAPC, TCTA and H2: HOMO levels + the optical gap
- HOMO levels of PO-T2T: UPS measurement
- LUMO levels of PO-T2T: CV measurement

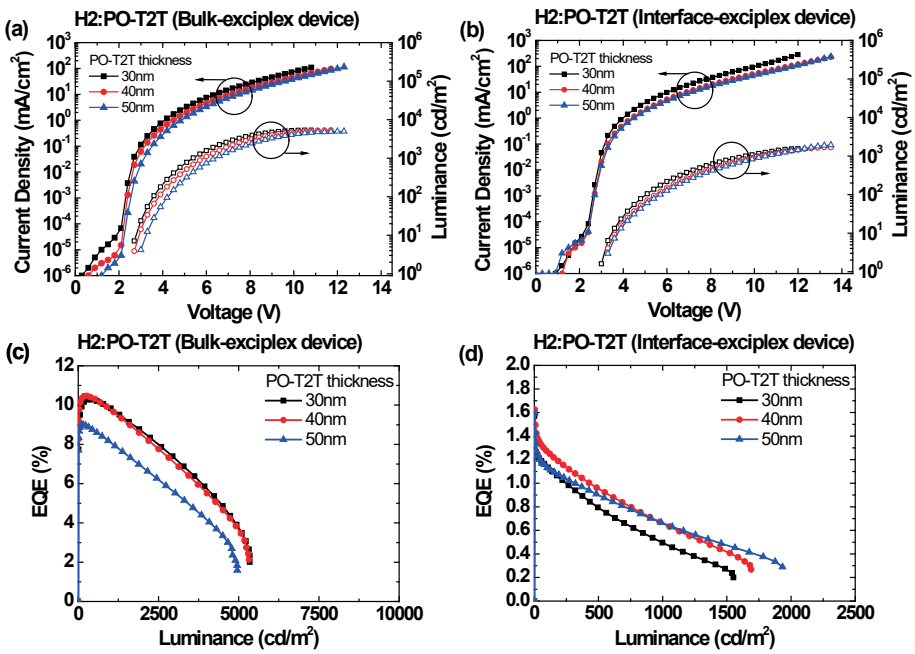

Figure 2.8 (a) Current density-voltage-luminance (*J-V-L*) characteristics of H2:PO-T2T bulk-exciplex OLEDs and (b) H2:PO-T2T interface-exciplex OLEDs (c) External quantum efficiencies (EQEs) versus luminance curves of H2:PO-T2T bulk-exciplex OLEDs and (d) H2:PO-T2T interface-exciplex OLEDs.

It should be noted that the maximum EQE increased by 1.4 times from 7.5% to 10.6% compared to H2:PO-T2T OLEDs that do not contain pure H2 (5 nm) layer between HTM and EML. This is presumably due to the decrease of the ratio of exciplexes formed at the interface with TCTA and the increase of H2:PO-T2T exciplex formation rates when the emission zone of the device moves toward HTM. Detailed characteristics of both devices are summarized in table 2.3.

Figure 2.9 represents the ratio of singlet excitons participating in luminescence. The devices were fabricated with an ETL thickness of 30 nm to 50 nm at 10 nm intervals. In the simulation, the charge balance was assumed to be 1. Normally in conventional fluorescent OLEDs, only about 25% of singlet excitons are known to be involved in luminescence. However in H2:PO-T2T exciplex system, experimentally obtained maximum EQE values indicate that at least 63% and at most 72% of the radiative singlet excitons (η_S) are involved in the luminescence when comparing the simulation results with experimental values. This is speculated as efficient triplet harvesting is possible by the delayed component in H2:PO-T2T exciplex system, thereby increasing the proportion of singlet excitons capable of emitting light.

Table 2.3 Device performance of H2:PO-T2T interface, bulk exciplex based OLEDs

Device	Voltage [V]		EQE [%]		Current efficiency [cd A^{-1}]		Power efficiency [lm W^{-1}]	
	Turn-on	1,000 cd m^{-2}	Max.	1,000 cd m^{-2}	Max.	1,000 cd m^{-2}	Max.	1,000 cd m^{-2}
Interface device	3.0/3.3/3.3	9.6/10.2/10.5	1.6/1.6/1.6	1.2/0.6/0.7	3.5/3.9/4.1	1.2/1.7/1.8	3.7/3.8/3.9	0.4/0.5/0.5
Bulk device	2.7/2.7/3.0	5.4/6.0/6.6	10.3/10.6/9.0	9.8/9.6/7.9	24.0/26.1/23.9	22.8/24.1/21.0	21.9/24.3/21.5	13.3/12.6/10.0

* Variation of ETL thickness **(30nm/40nm/50nm)** while HTL thickness fixed as 50nm.

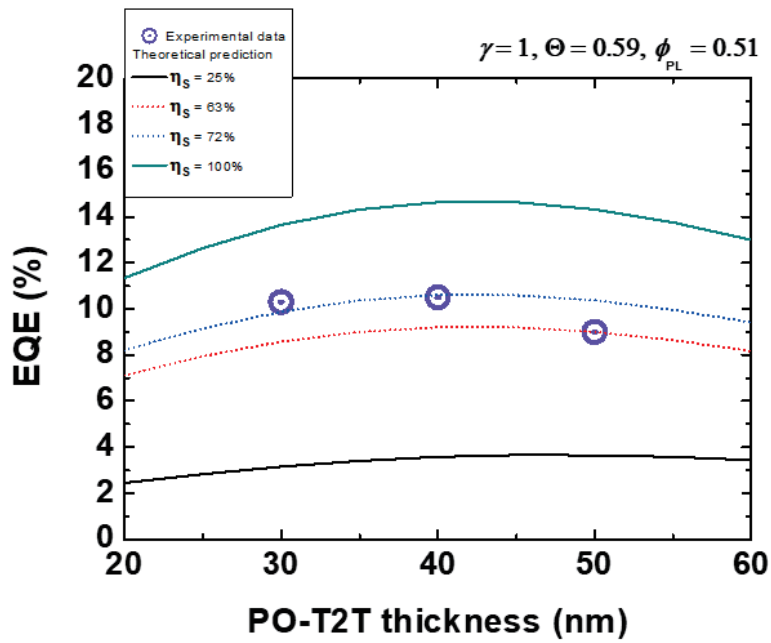

Figure 2.9 Air mode analysis of H2:PO-T2T exciplex forming co-host based OLEDs depending on PO-T2T (ETL) thickness while TAPC thickness fixed as 50nm. The device structure described in Figure 2.7b is used for the simulation.

The EL spectra of fabricated OLEDs are shown in figure 2.10a and 2.10b. Figure 2.10c and 2.10d show the *J-V-L* characteristics and current efficiency, power efficiency plot of OLEDs. I tried to observe whether the EL spectra red-shift phenomena is reversible or not. The first measurement was conducted from 3 V to 6 V, and the second measurement was taken after 5 minutes from 3 V to 13.5 V. Regardless of the first and second measurements, both interface-exciplex and bulk-exciplex devices showed that the EL spectra red-shift started from the same initial peak wavelength. All of these situations prove that this phenomenon is reversible due to its own characteristic of H2:PO-T2T exciplex.

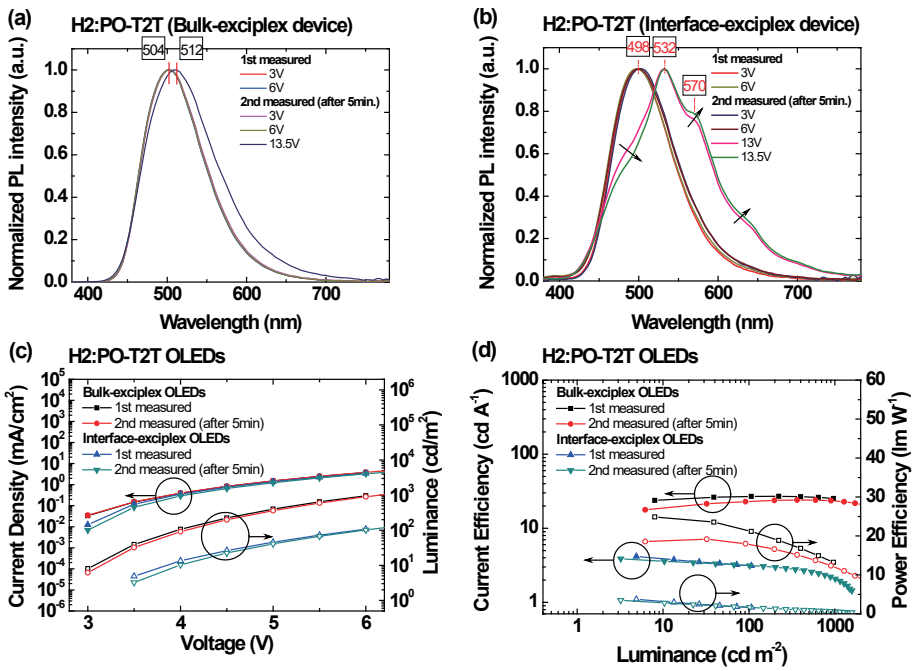

Figure 2.10 (a) EL spectra of H2:PO-T2T bulk-exciplex OLEDs. The first measurement was conducted from 3 V to 6 V, and the second measurement was taken after 5 minutes interval from 3 V to 13.5 V. (b) H2:PO-T2T interface-exciplex OLEDs. (c) Current density-voltage-luminance (*J-V-L*) characteristics of H2:PO-T2T bulk-exciplex and interface-exciplex OLEDs (d) Current efficiency and power efficiency of the OLEDs

2.4 Conclusion

In this chapter, I introduced novel greenish-blue exciplex system with high delayed emission components ($k_{ISC} \times k_{RISC}$, Φ_d). OLEDs with 7.5% maximum EQE were fabricated using H2:PO-T2T exciplex system. To reduce the formation of the interface exciplex in H2:PO-T2T OLED, a 5nm pure H2 layer was inserted between HTM and EML. As a result, a device with a maximum EQE of 10.6% has been fabricated, and this result is 1.4 times better than the previous device. This finding suggests that the insertion of a buffer layer between EML and HTM or ETM has a possibility of increasing the exciplex formation, leading to increased efficiency. Also, maximum EQE value indicates that at least 63% and at most 72% of the radiative singlet excitons (η_s) are involved in the luminescence when comparing the simulation results with experimental values.

Another interesting point was the EL spectra showed a tendency to red-shift (reversible reaction) depending on the applied voltage increment. This phenomenon was assumed as the intrinsic properties of the H2:PO-T2T exciplex or consisting materials.

Chapter 3. Yellow Fluorescent Organic Light-Emitting Diodes with extended lifetime and low efficiency roll-off using H2:PO-T2T exciplex as host

3.1 Introduction

During few decades, organic light-emitting diodes (OLEDs) has been improved very rapidly due to advent of new generations of OLEDs which has own advantages suggesting a breakthrough solution for achieving a theoretical limit of EQE and device stability. Fluorescent OLED is one representative of the 1st generation of OLEDs. Fluorescent OLEDs have advantages such as low cost, long operational lifetime, and fast exciton decay rate. The main important point of fluorescent OLEDs is, how to transfer energy efficiently from host to dopant preserving more radiative excitons for better efficiency and optimization of a device structure for device stability. In general, only 25% of singlet excitons are known to participate in luminescence, which shows theoretical limit. To overcome the theoretical limit, researchers have been actively focused

on the selection of host materials or sensitizer. Exciplex hosts can be one of the candidates as a sensitizer for fluorescent OLEDs which composed of a hole transporting material (HTM) and electron transporting material acting as a bipolar host. As exciplex is expected to have small ΔE_{ST} which enables efficient reverse intersystem crossing (RISC) process, then additional triplet excitons can be harvest to singlet excitons in the delayed emission process. These additional excitons can be transferred from exciplex to the dopant through the Förster energy transfer process which influences an additional portion for maximum EQE. Sensitization concept has been widely used to overcome the theoretical limit, then reached the EQE over 30% using TADF materials as host or sensitizers recently in fluorescent OLEDs.[83,84]

There have been many reports of yellow fluorescent OLEDs based on exciplex system.[13,67-68,81-84] Few studies have focused on achieving high EQE and device stability. However, in the lifetime aspect, we still need to progress in conventional fluorescent OLEDs.

In this chapter, a yellow fluorescent OLED with extended operational lifetime, low operational voltage and efficiency roll-off was reported. This work presents fluorescent OLED based on a new exciplex-forming co-host consisting of a hole-transporting material [8,8′-

spirobi[indolo(3,2,1-de)acridine] (H2)], and an electron-transporting material containing phosphine oxide and triazine core structure [(1,3,5-triazine-2,4,6-triyl)tris(benzene-3,1-diyl)]tris(diphenylphosphine oxide) (PO-T2T)] with high delayed emission, including (Φ_{ISC} x Φ_{RISC}, Φ_d) kinetic constants, doped with yellow fluorescent dye: [2,8-di(*t*-butyl)-5,11-di[4-(*t*-butyl)phenyl]-6,12-diphenylnaphthacene (TBRb)]. The yellow fluorescent OLED based on H2:PO-T2T exciplex forming co-host has a maximum EQE of 7.2%, a current efficiency (CE) of 21.8 cd A^{-1} and power efficiency (PE) of 25.3 lm W^{-1} with low operating voltage 2.7 V and EQE roll-off. Furthermore, the device using the H2:PO-T2T exciplex doped with TBRb as EML, has an LT_{50} of 60 hours at 1,000 cd m^{-2}. This operational lifetime result is higher than previously reported exciplex based fluorescent OLEDs such as TCTA:B4PYMPM:TBRb, without phosphorescent sensitizer.[13]

3.2 Experimental

3.2.1 Organic film fabrication

To fabricate organic film samples, cleanly washed quartz substrates should be prepared after the piranha treatment. The way to dissolve the solution for the piranha treatment is to mix sulfuric acid (H_2SO_4) and hydrogen peroxide (H_2O_2) in a 3:1 ratio. The piranha process is done by dipping the substrate in the piranha solution for at least 1hour and 30 minutes and rinsing with deionized water. After piranha treatment, all substrates were cleaned using isopropyl alcohol and acetone inside of a bath to remove remains. The organic layers were deposited on the quartz substrate by the thermal vacuum-evaporation process under a pressure of 6×10^{-8} Torr. Metal masks were used to form an active area of 2×2 mm^2 and to fabricate various conditions. In a single material layer was deposited at a rate of 1 Å/s and the deposition rate of the co-deposited layers was 1 Å/s in total, which was calculated in proportion to the molar mass of composing materials.

3.2.2 Device fabrication

To fabricate exciplex OLEDs, the organic layers and aluminum (used as the cathode) were deposited on top of 70-nm-thick indium tin oxide (ITO) by the thermal vacuum-evaporation process under a pressure of $< 7.6\times10^{-8}$ Torr. Metal masks were used to form an active area of 2×2 mm^2 and to fabricate various conditions. Before deposition, all 70-nm-thick ITO substrates were pre-heated at 250 ℃ for 30 minutes and rinsed with deionized water. After the rinsing process, all substrates were pre-cleaned using isopropyl alcohol and acetone inside of a bath to remove remains. Next, the substrates were exposed under a UV-ozone flux for an overall 6 minutes. (1 minute 30 seconds for nitrogen, oxygen each and 3 minutes for UV light) In a single material layer was deposited at a rate of 1 Å/s and the deposition rate of the co-deposited layers was 1 Å/s in total, which was calculated in proportion to the molar mass of composing materials. The deposition rate of aluminum (used as an electrode) was 4 Å/s. The fabricated devices were encapsulated with a cover glass using UV-curable resin in a glovebox before the measurement of device properties.

3.2.3 Photophysical properties of an organic film

The Absorption spectrum of [2,8-di(*t*-butyl)-5,11-di[4-(*t*-butyl)phenyl]-6,12-diphenylnaphthacene (TBRb)] was measured using Cary 5000 UV-vis-NIR (Agilent Technologies) spectrophotometer. The TBRb solution was prepared by dissolving the TBRb material at a concentration of 10^{-5}M in methylene chloride solvent.[13] The PL spectra of organic films were measured using a spectrofluorometer (Photon Technology International) connected to a monochromator (Acton Research). The excitation wavelength of xenon-lamp was fixed as 325nm for H2, PO-T2T neat film, H2:PO-T2T mixed film, and H2:PO-T2T:TBRb doped film. To measure the PL efficiency, organic materials were deposited on quartz substrates in 30-nm thickness. 6-inches diameter integrating sphere (Labsphere Co.), pasted with barium sulfate ($BaSO_4$) was served as a darkroom for measuring accurate efficiency value, and a monochromator (Acton Research Co.) attached to a photomultiplier tube (Hamamatsu Photonics K.K.) was used as the optical detection system. Detailed experimental information for calculation of PL efficiency value is described in previously reported papers.[71,72,73] To measure the transient PL signals, nitrogen laser (337 nm)

was used as the excitation light source, and a streak camera (Hamamatsu Photonics) was used as the optical detection system. Angle-dependent PL (ADPL) experiment was performed using a fiber optic spectrometer (Ocean Optics Maya2000). ADPL measurement behaved on automatically rotating stages and half-cylinder lens. The organic film attached to a half-cylinder lens without any refractive index difference using index matching oil. Detailed experimental information for the experimental setup is described in previously reported papers. [2,34,74-75]

3.2.4 Device characterization

Current density, luminance, and EL spectra were measured using a programmable source meter (Keithley 2400) and a radiometer (SpectraScan PR650). The EQEs and power efficiency of OLEDs were obtained from overall data of current density-voltage-luminance (*J-V-L*) characteristics, EL spectra, and Lambertian correction factors. Device lifetime was measured using (Polaronix M6000T) device operation system. A current depending on initial luminance of 1,000 cd m^{-2} was applied to the device until it reached 50% of the initial luminance.

3.3 Result and discussion

Based on previously reported exciplex in chapter 2 which shown about 12 powers of 10 delayed kinetic constant ($k_{ISC} \times k_{RISC}$) and EL spectra red-shift occurs while applying voltage increment, I expect better EQE and device stability if it applied to fluorescent OLEDs due to better photoluminescence quantum yield and fixed EL spectra. Figure 3.1 depicts the overall excited-state process while transferring energy from exciplex to conventional fluorescent dye.

[8,8′-spirobi[indolo(3,2,1-de)acridine] (H2)] was selected as donor material and [(1,3,5-triazine-2,4,6-triyl)tris(benzene-3,1-diyl)]tris(diphenylphosphine oxide) (PO-T2T)] was selected as acceptor material to form an exciplex. [2,8-di(*t*-butyl)-5,11-di[4-(*t*-butyl)phenyl]-6,12-diphenylnaphthacene (TBRb)] known to have high PLQY[10,13,85] was used as a conventional fluorescent emitter. Figure 3.2a shows the chemical structures of the materials used in the devices (EML) the highest occupied molecular orbital (HOMO), lowest unoccupied molecular orbital (LUMO) energy levels.[61,76,78]

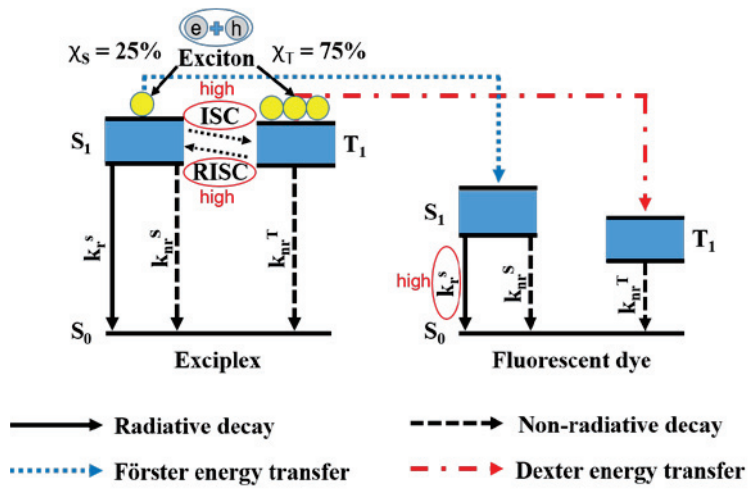

Figure 3.1 Schematic illustration of the excited-state process while transferring energy from exciplex to conventional fluorescent dye.

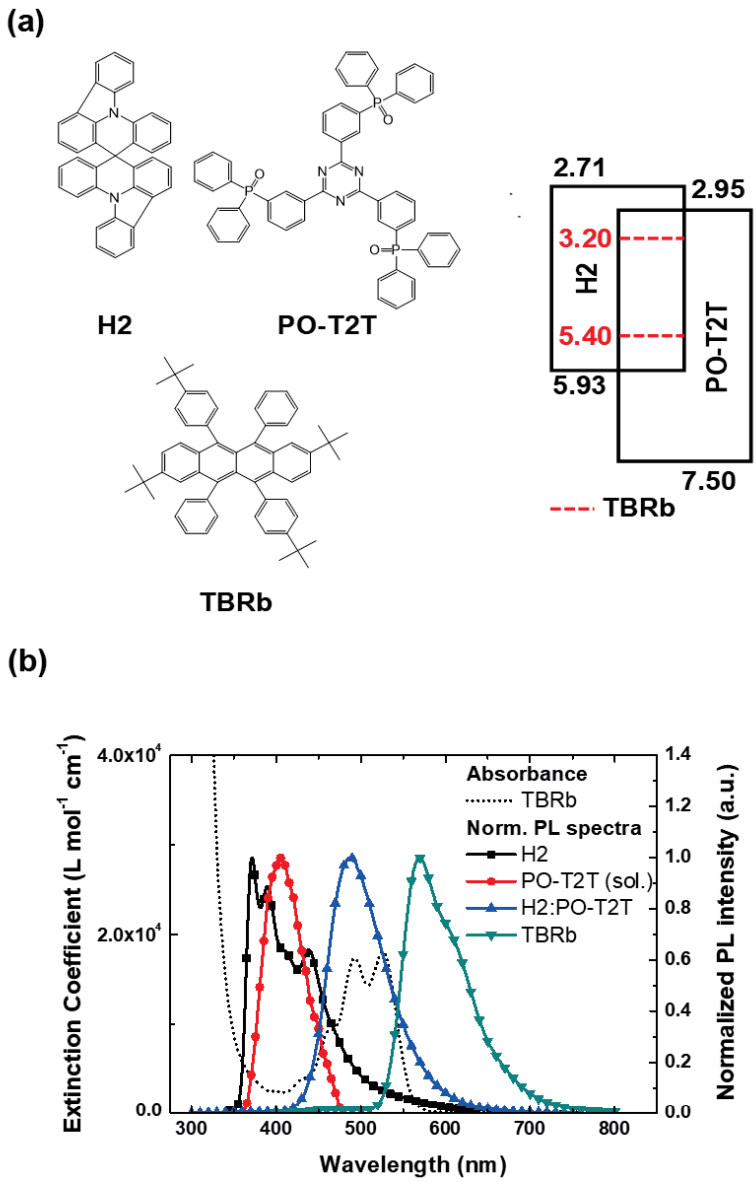

Figure 3.2 (a) Molecular structure and energy levels of the exciplex-forming host and fluorescent emitter. (b) The room-temperature absorption spectrum of TBRb (short dot) and PL spectra of H2 (line with rectangulars), PO-T2T (line with circles), and co-deposited H2:PO-T2T (line with upward triangles) 30nm-thick thin film and TBRb (line with downward triangles).

Figure 3.2b shows an absorption spectrum of TBRb and the PL spectra of H2, PO-T2T neat film, H2:PO-T2T (molar ratio of 1:1) co-deposited film. The large spectral overlap between the absorption spectrum of TBRb and the PL spectrum of the H2:PO-T2T exciplex, meaning efficient Förster energy transfer occurs from exciplex to the singlet of TBRb. The Förster radius from H2:PO-T2T exciplex to the TBRb dopant was calculated as 4.6 nm. Figure 3.3a shows the PL spectra of 0.5wt%, 1wt%, 2wt% TBRb doped in the H2:PO-T2T-mixed co-host 30 nm-film. As the concentration of TBRb doping was increased, exciplex emission gradually decreased, indicating that energy transfer from exciplex to TBRb occurred efficiently. The PLQYs of the three films were 45% (with 0.5wt TBRb), 52% (with 1wt% TBRb), 57% (with 2wt% TBRb) and emission peak at 565nm, emitting dipole orientation (Θ) value is well fitted by a horizontal-to-vertical dipole ratio TBRb h:v = 0.84:0.16 indicating the emitting dipole orientation results match with the previously reported TBRb dopant properties.[10,13,85]

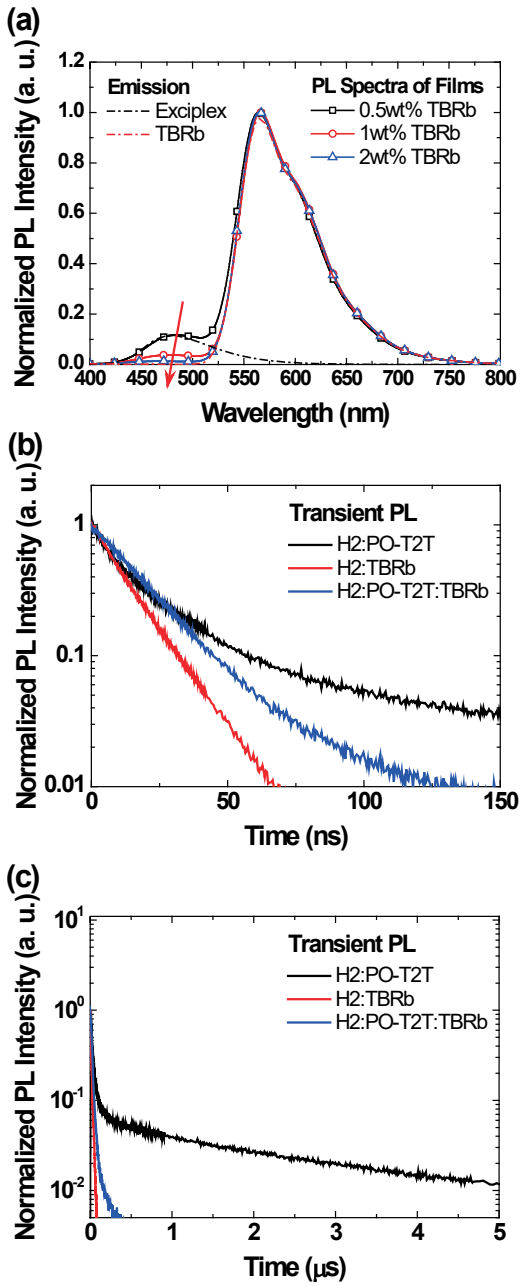

Figure 3.3 (a) PL spectra of 0.5, 1, 2wt% TBRb doped in the H2:PO-T2T-mixed film. (b) Transient PL of the H2:PO-T2T mixed film, TBRb doped in H2 film and the H2:PO-T2T:2wt% TBRb film (x-axis: nanoseconds scale) (c) Transient PL decay curves in microseconds scale

To confirm the energy transfer process between exciplex and fluorescent dopant, I measured transient PL. Figure 3.3b and Figure 3.3c show the transient PL data of the H2:PO-T2T mixed film, TBRb doped in H2 film and the H2:PO-T2T:2wt% TBRb film. Every film doped with the fluorescent dopant shows that the radiative decay rate decreased to several hundred nanoseconds. Also, more delayed fluorescence was observed in TBRb doped in H2:PO-T2T exciplex film than TBRb doped in neat H2 film. This suggests that additional fluorescence can affect the efficiency of the device.

To identify the effect of the fluorescent dopant, an OLED was fabricated based on H2:PO-T2T exciplex co-host and TBRb as an emitter. The schematic diagram of the device structure and the energy levels of the consisting layers are shown in Figure 3.4a. The device structure of fluorescent OLED was same as follows; ITO (70 nm) / TAPC (65 nm) / TCTA (10 nm) / H2 (5 nm) / H2:PO-T2T:2wt% TBRb (30 nm) / PO-T2T (65nm) / LiF (1 nm) / Al (100 nm). 1,1-Bis[(di-4-tolylamino)phenyl]cyclohexane (TAPC) and 4,4′,4″-Tris(carbazol-9-yl)triphenylamine (TCTA) were selected as hole-transport material (HTM) in OLED devices.

It's high ionization potential (IP=5.6V, 5.8V) and hole mobility shows good hole injection and transport properties widely used.[86,87] Fabricated device shows EL emission peak at 565nm indicating efficient Förster energy transfer to TBRb. (Figure 3.4b)

The current density-voltage-luminance (*J*-*V*-*L*) characteristics of the exciplex OLED and exciplex-based conventional fluorescent OLED at room temperature are shown in Figure 3.4c. Both devices showed a turn-on voltage of 2.7V. The EQEs and luminance of the devices are displayed in Figure 3.4d. The maximum efficiency of the fluorescent OLEDs was 7.2% with yellow emission.

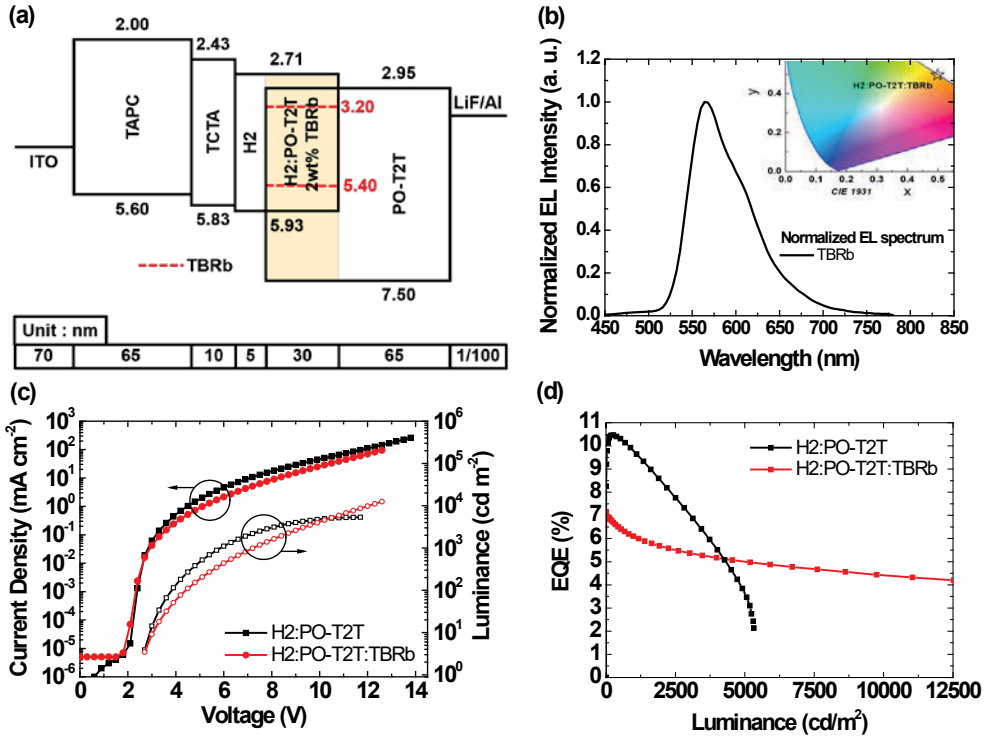

Figure 3.4 (a) Schematic diagram of the fluorescent device structure and energy levels of the consisting layers of H2:PO-T2T:TBRb fluorescent OLEDs (b) Electroluminescence (EL) spectra at 1,000 cd m^{-2}. (c) Current density-voltage-luminance (*J-V-L*) characteristics of H2:PO-T2T and H2:PO-T2T:TBRb OLEDs (d) External quantum efficiencies (EQEs) versus luminance curves of H2:PO-T2T and H2:PO-T2T:TBRb OLEDs

- Every substrate was annealed at 250 °C for 30min before evaporation
- Energy levels were determined by CV or UPS.
- HOMO levels of TAPC, TCTA and H2: CV measurement
- LUMO levels of TAPC, TCTA and H2: HOMO levels + the optical gap
- HOMO levels of PO-T2T: UPS measurement
- LUMO levels of PO-T2T: CV measurement

Table 3.1 Device performances of fluorescent OLED compared with exciplex forming co-host based OLED reported in chapter 2

Device	Voltage [V]			EQE [%]			Power Efficiency [lm W^{-1}]		
	Turn-on	1,000 cd m^{-2}	10,000 cd m^{-2}	Max.	1,000 cd m^{-2}	10,000 cd m^{-2}	Max.	1,000 cd m^{-2}	10,000 cd m^{-2}
Exciplex	2.7	5.7	-	10.6	9.9	-	24.3	13.1	-
TBRb	2.7	7.2	12.0	7.2	6.1	4.5	25.3	8.3	3.7

As refer to EQEs of fluorescent OLEDs as a function of luminance (figure 3.4d), comparing the EQE values at 5,000 cd m^{-2} from the maximum EQE, data shows a decrease about 31% from 7.2% to 5% for fluorescent OLEDs and a 65% reduction from 10.6% to 3.8% for exciplex-based OLEDs. These prove efficiency roll-off decreased in fluorescent OLEDs compared with H2:PO-T2T exciplex OLEDs. Detailed characteristics of the device are summarized in table 3.1.

Figure 3.5a shows the decay of the EL intensity of the OLEDs as a function of operating time under constant current at an initial luminance (L_0) of 1,000 cd m^{-2}. Although 312.7 h of a lifetime has been reported in 2017, based on TCTA:B4PYMPM exciplex with $Ir(ppy)_3$ as a sensitizer and TBRb as a fluorescent dopant, I only focused on comparing conventional fluorescent OLEDs based on exciplex as host from the previous result.[13] The LT_{50} lifetime of the yellow fluorescent OLEDs was 60 h at 1,000 cd m^{-2} in TBRb doped with H2:PO-T2T exciplex system. This result is about 8.5 times better than TBRb doped with TCTA:B4PYMPM exciplex system and 1,000 times better than H2:PO-T2T exciplex forming co-host based OLEDs.[13]

I assumed this prolonged lifetime comes from fixed EL spectra compared with H2:PO-T2T exciplex-based OLEDs and reduced exciton radiative decay rate constant from transient PL data.

To analyze the reason for an extended lifetime in H2:PO-T2T:TBRb fluorescent OLEDs, I compared transient PL data between TBRb doped in H2:PO-T2T exciplex and TCTA:B4PYMPM exciplex. (Figure 3.5b) Since the prompt radiative decay rate of H2:PO-T2T:TBRb is faster than TCTA:B4PYMPM:TBRb, it could be assumed that the time for exciton remains in the excited state is reduced, and the proportion of degradation products produced in the excited state is reduced, resulting in a relatively extended lifetime.

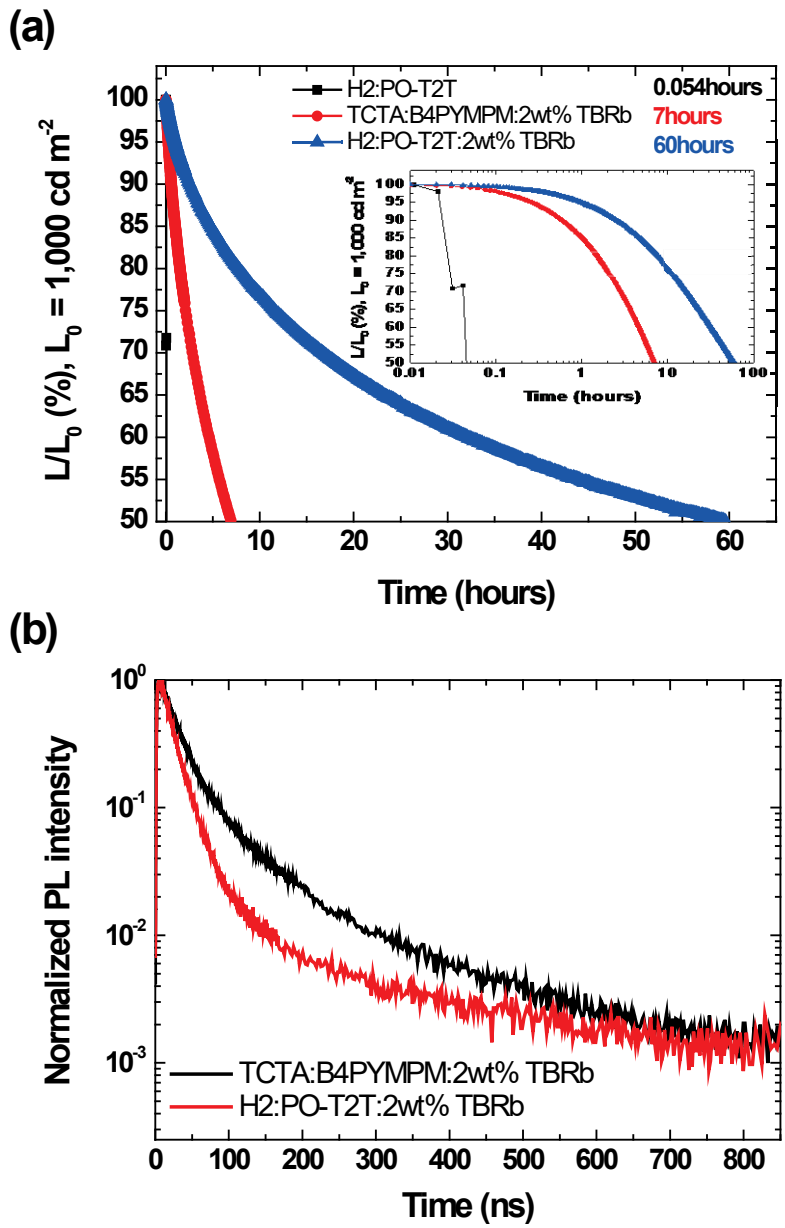

Figure 3.5 (a) Operational lifetime of OLEDs at an initial luminance (L_0) of 1,000 cd m^{-2}. (b) Comparison of transient PL data between TBRb doped in different exciplex. TCTA:B4PYMPM exciplex (black line), H2:PO-T2T exciplex (red line).

3.4 Conclusion

I fabricated yellow fluorescent OLEDs with fixed EL peak wavelength (595nm). The fluorescent OLEDs based on H2:PO-T2T exciplex shows improved efficiency roll-off compared with H2:PO-T2T exciplex based-OLEDs. The LT_{50} lifetime of the yellow fluorescent OLEDs was 60 h at 1,000 cd m^{-2} in TBRb doped with H2:PO-T2T exciplex system. This result is about 8.5 times better than TBRb doped with TCTA:B4PYMPM exciplex system and 1,000 times better than H2:PO-T2T exciplex OLEDs.

Chapter 4. Blue Fluorescent Organic Light-Emitting Diodes based on blue exciplex forming co-hosts

4.1 Introduction

Efficient blue exciplex-forming co-host based organic light-emitting diodes (OLEDs) with device stability are still challenging issues since it has been actively researched after the 20th century.[91,92,93] To obtain better efficiency, thermally activated delayed fluorescence (TADF) materials were reported and used for efficient triplet harvesting via reverse intersystem crossing (RISC) process.[97-105] Exciplex or TADF molecule can be one of the host candidates which has a small singlet-triplet energy difference(ΔE_{ST}). However, still efficient blue OLEDs with the stable blue-exciplex system has been reported rarely compared to the years studied.[14,19,61,78,94-96]

For better efficiency and operational stability in blue OLEDs, the sensitization concept has been widely used for harvesting additional radiative excitons that contribute to efficiency increment. The use of

TADF sensitizers has proven highly successful in recent years, showing efficient blue fluorescent OLEDs with external quantum efficiencies (EQEs) up to 18.8%.[10,14,106-109] However, still exciplex forming co-host based fluorescent OLEDs are rarely reported. In this work, I wanted to fabricate conventional fluorescent OLEDs based on a blue exciplex-forming co-host.

This work presents blue fluorescent OLEDs with extended operational lifetime based on novel blue exciplex-forming co-host consisting of a hole-transporting material [9-(4-(9*H*-pyrido[2,3-*b*]indol-9-yl)phenyl)-9*H*-3,9′-bicarbazole] (pBCb2Cz)] and an electron-transporting material containing phosphine oxide [(2,6-bis(4-(diphenylphosphoryl)-phenyl)-pyridine) (BM-A11)] doped with two different blue fluorescent dyes: [2,5,8,11-Tetra-*tert*-butylperylene (TBPe)] and [N1,N6-bis(5-(tert-butyl)-2-methylphenyl)-N1,N6-bis(2,5-dimethylphenyl)-pyrene-1,6-diamine (MBD105)].[10,14,89,90] The name of MBD105 referred from [N1,N6-bis(5-(tert-butyl)-2-methylphenyl)-N1,N6-bis(2,5-dimethylphenyl)-pyrene-1,6-diamine (3Me-1Bu-TPPDA) (MBD106)] reported by Jong wook Park's group in 2018, also MBD105 synthesized by the same group. [88]

The blue fluorescent OLEDs with the pBCb2Cz:BM-A11

exciplex host has a maximum EQE of 5.22%, 4.81% and a current efficiency (CE) of 7.85cd A^{-1}, 6.25cd A^{-1} with low operating voltages of 3.00, 3.30V each. More importantly, the fluorescent devices based on the pBCb2Cz:BM-A11 exciplex host shows extended operational lifetime LT_{50} of 0.44hours, 2.7hours at 400 cd m^{-2}. Also fluorescent OLEDs show EL peak wavelength (λ_{max}^{EL} : 464nm / 464nm) and color coordinate (CIE *x*, CIE *y*: 0.1329, 0.2225 / 0.1302, 0.1770) which results are well-matched with blue emission with y-axis close to 0.2.

The deep blue emission is defined as having a CIE coordinate $y < 0.15$ along with $x + y < 0.30$.[80] The color coordinate of fabricated devices are $x + y < 0.30$ for exciplex OLEDs which showing deep-blue emission and $x + y < 0.35$, $x + y < 0.31$ for blue-fluorescent OLEDs each. These are important because having possibility for stable highly efficient full-color display and high color render index (CRI) white OLED (WOLEDs).[80]

4.2 Experimental

4.2.1 Organic film fabrication

To fabricate organic film samples, cleanly washed quartz substrates should be prepared after the piranha treatment. The way to dissolve the solution for the piranha treatment is to mix sulfuric acid (H_2SO_4) and hydrogen peroxide (H_2O_2) in a 3:1 ratio. The piranha process is done by dipping the substrate in the piranha solution for at least 1hour and 30 minutes and rinsing with deionized water. After piranha treatment, all substrates were cleaned using isopropyl alcohol and acetone inside of a bath to remove remains. The organic layers were deposited on the quartz substrate by the thermal vacuum-evaporation process under a pressure of 2×10^{-7} Torr. Metal masks were used to form an active area of 2×2 mm^2 and to fabricate various conditions. In a single material layer was deposited at a rate of 1 Å/s and the deposition rate of the co-deposited layers was 1 Å/s in total, which was calculated in proportion to the molar mass of composing materials.

4.2.2 Device fabrication

To fabricate exciplex OLEDs, the organic layers and aluminum (used as the cathode) were deposited on top of 70-nm-thick indium tin oxide (ITO) by thermal vacuum-evaporation under a pressure of 8.6×10^{-8} Torr. Metal masks were used to form an active area of 2×2 mm^2 and to fabricate various conditions. Before deposition, all 70-nm-thick ITO substrates were pre-heated at 250 ℃ for 30 minutes and rinsed with deionized water. After the rinsing process, all substrates were pre-cleaned using isopropyl alcohol and acetone inside of a bath to remove remains. Next, the substrates were exposed under a UV-ozone flux for 6 minutes. (1 minute 30 seconds for nitrogen, oxygen each and 3 minutes for UV light) In a single material layer was deposited at a rate of 1 Å/s and the deposition rate of the co-deposited layers was 1 Å/s in total, which was calculated in proportion to the molar mass of composing materials. The deposition rate of aluminum (used as an electrode) was 4 Å/s. The fabricated devices were encapsulated with a cover glass using UV-curable resin in a glovebox before the measurement of device properties.

4.2.3 Photophysical properties of an organic film

The Absorption spectra of [2,5,8,11-Tetra-*tert*-butylperylene (TBPe)] and [N1,N6-bis(5-(tert-butyl)-2-methylphenyl)-N1,N6-bis(2,5-dimethylphenyl)-pyrene-1,6-diamine (MBD105)] were measured using Cary 5000 UV-vis-NIR (Agilent Technologies) spectrophotometer. TBPe, MBD105 solutions were prepared by dissolving materials at a concentration of 10^{-5}M in methylene chloride solvent.[14] Also, the Absorption spectra of organic films were measured using Cary 5000 UV-vis-NIR (Agilent Technologies) spectrophotometer. The PL spectra of organic films were measured using a fiber optic spectrometer (Ocean Optics Maya 2000) as the optical detection system. The excitation wavelength of He-Cd laser was set as 325nm for pBCb2Cz, BM-A11 neat film, pBCb2Cz:BM-A11 mixed film and pBCb2Cz:BM-A11:TBPe, pBCb2Cz:BM-A11:MBD105 doped films. To measure the PL efficiency, organic materials were deposited on quartz substrates in 30-nm thickness. 6-inches diameter integrating sphere (Labsphere Co.), pasted with barium sulfate ($BaSO_4$) was served as a darkroom for measuring accurate efficiency value, and a monochromator (Acton Research Co.) attached to a photomultiplier tube (Hamamatsu Photonics K.K.) was used as the

optical detection system. Detailed experimental information for calculation of PL efficiency value is described in previously reported papers.[71,72,73] To measure the transient PL signals, nitrogen laser (337 nm) was used as the excitation light source, and a streak camera (Hamamatsu Photonics) was used as the optical detection system. Angle-dependent PL (ADPL) experiment was performed using a fiber optic spectrometer (Ocean Optics Maya2000). ADPL measurement behaved on automatically rotating stages and half-cylinder lens. The organic film attached to a half-cylinder lens without any refractive index difference using index matching oil. Detailed experimental information for the experimental setup is described in previously reported papers. [2,34,74-75]

4.2.4 Device characterization

Current density, luminance, and EL spectra were measured using a programmable source meter (Keithley 2400) and a radiometer (SpectraScan PR650). The EQEs and power efficiency of OLEDs were obtained from overall data of current density-voltage-luminance (*J-V-L*) characteristics, EL spectra, and Lambertian correction factors. Device lifetime was measured using (Polaronix M6000T) device operation system. A current depending on initial luminance of 400 cd m^{-2} was applied to the device until it reached 50% of the initial luminance.

4.3 Result and discussion

Figure 4.1a shows the molecular structures of the compounds used in the devices (EML), the highest occupied molecular orbital (HOMO), lowest unoccupied molecular orbital (LUMO), and triplet energy levels. [9-(4-(9*H*-pyrido[2,3-*b*]indol-9-yl)phenyl)-9*H*-3,9′-bicarbazole] (pBCb2Cz)] was selected as donor material and [(2,6-bis(4-(diphenylphosphoryl)-phenyl)-pyridine) (BM-A11)] was selected as acceptor material to form an exciplex. Two kinds of blue fluorescent materials were used as emitters: [2,5,8,11-Tetra-*tert*-butylperylene (TBPe)] and [N1,N6-bis(5-(tert-butyl)-2-methylphenyl)-N1,N6-bis(2,5-dimethylphenyl)-pyrene-1,6-diamine (MBD105)].[10,14,89,90] Figure 4.1b shows absorption spectra of fluorescent emitters: TBPe, MBD105 and the PL spectra of pBCb2Cz, BM-A11 neat film, pBCb2Cz:BM-A11 (molar ratio of 1:1) co-deposited film, and TBPe, MBD105 doped films. The large spectral overlap between the absorption spectra of TBPe, MBD105 and the PL spectra of the pBCb2Cz:BM-A11 exciplex, indicating the possibility of efficient Förster energy transfer from exciplex to the singlet of fluorescent emitters. The Förster radius from pBCb2Cz:BM-A11

exciplex to TBPe, MBD105 dopants were calculated as 4.30 nm, 4.14 nm each.

The PLQY and emitting dipole orientation was also observed because those are influencing factors in device characteristics such as EQE. Each values are summarized in table 4.1 and figure 4.2. pBCb2Cz:BM-A11 shows 12% PLQY value and pBCb2Cz:BM-A11:1wt% TBPe, pBCb2Cz:BM-A11:5wt% MBD105 shows 68%, 48% each. The Emitting dipole orientation of pBCb2Cz:BM-A11, pBCb2Cz:BM-A11:1wt% TBPe and pBCb2Cz:BM-A11:5wt% MBD105 were analyzed using the angle-dependent PL intensity. The experimental data are well fitted by a horizontal-to-vertical dipole ratio of h:v = 0.66:0.34 for pBCb2Cz:MB-A11, h:v = 0.74:0.26 for TBPe and h:v = 0.86:0.14 for MBD105 indicating that the transition dipole moments have a preferred orientation in horizontal direction.

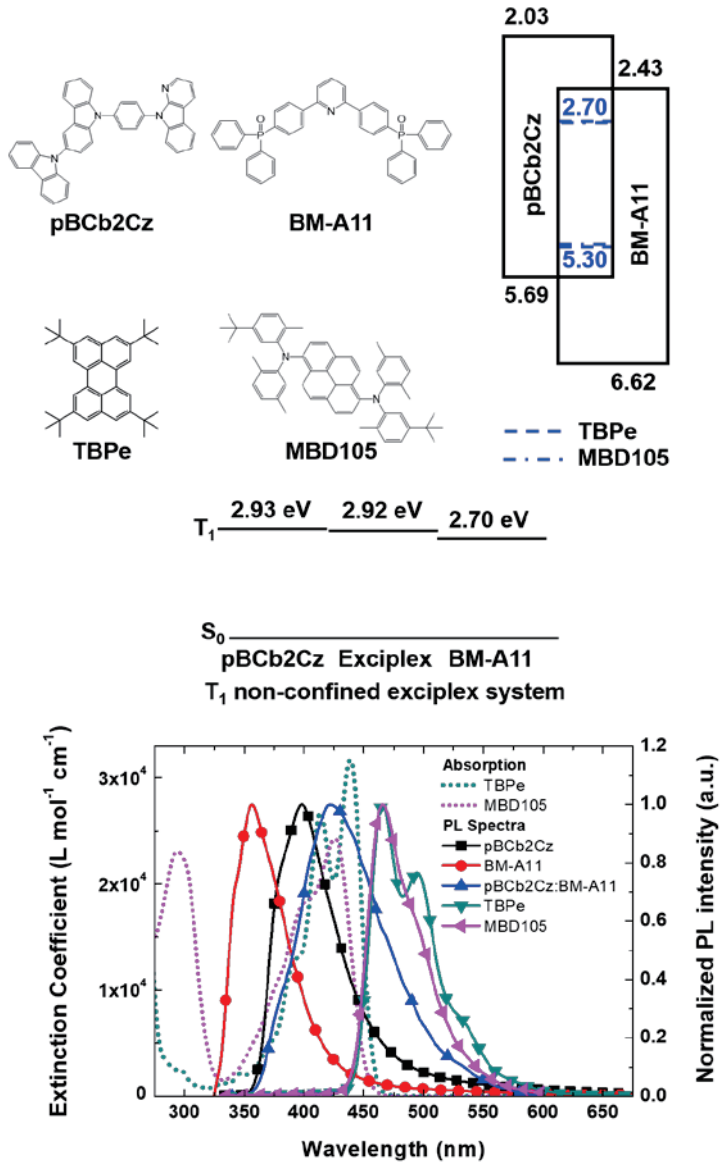

Figure 4.1 (a) Molecular structures of the host (pBCb2Cz, BM-A11) and fluorescent dopants (TBPe, MBD105) with energy levels (b) Absorption and normalized photoluminescence (PL) spectra of pBCb2Cz (line with squares), BM-A11 (line with circles), pBCb2Cz:BM-A11 co-deposited thin films (line with upward triangles), pBCb2Cz:BM-A11:1wt% TBPe (line with downward triangles), pBCb2Cz:BM-A11:5wt% MBD105 (line with leftward triangles).

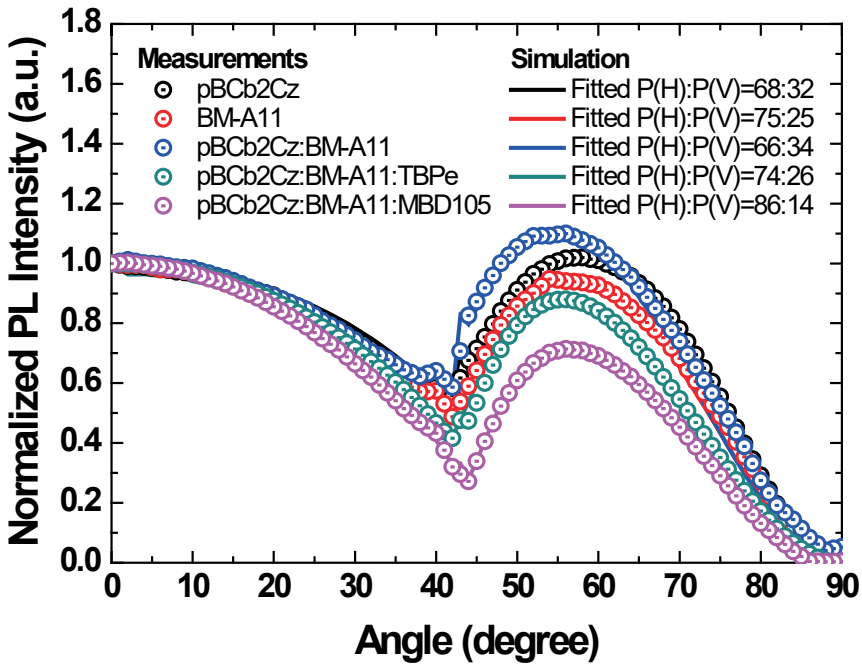

Figure 4.2 Experimentally obtained angle-dependent PL intensity of the *p*-polarized light emitted from a 30 nm-thick pBCb2Cz:BM-A11, pBCb2Cz:BM-A11:1wt% TBPe and pBCb2Cz:BM-A11:5wt% MBD105 films

Table 4.1 Optical properties of pBCb2Cz:BM-A11 exciplex and fluorescent emitters

Optical properties of pBCb2Cz:BM-A11 exciplex with fluorescent emitters									
Exciplex system	**Fluorescent Dopants**	**Color**	**PLQY (%)**			**Θ (%)**			**λ_{max}^{PL} (nm)**
			Donor	**Acceptor**	**Exciplex**	**Donor**	**Acceptor**	**Exciplex**	
pBCb2Cz:BM-A11	None	Blue	24	42	12	68	75	66	425
	1wt% TBPe		68			74			467
	5wt% MBD105		48			86			465

I measured the transient PL to identify the energy transfer process. Figure 4.3a and figure 4.3b show the transient PL of the exciplex emission integrated from 400nm to 600nm. The decay rate of the exciplex emission was faster when 1wt% TBPe and 5wt% MBD105 was doped in pBCb2Cz:BM-A11 exciplex indicating effective energy transfer occurred. While the decay curve shows single-exponential decay in pBCb2Cz:1wt% TBPe, pBCb2Cz:5wt% MBD105 case, fluorescent emitters doped in exciplex film shows more delayed fluorescence. This suggests the possibility of additional fluorescence resulted from delayed components of PL. As referred to transient PL data, figure 4.3c and figure 4.3d suggest that the emission of fluorescent doped films originated from each dopant through the efficient energy transfer process.

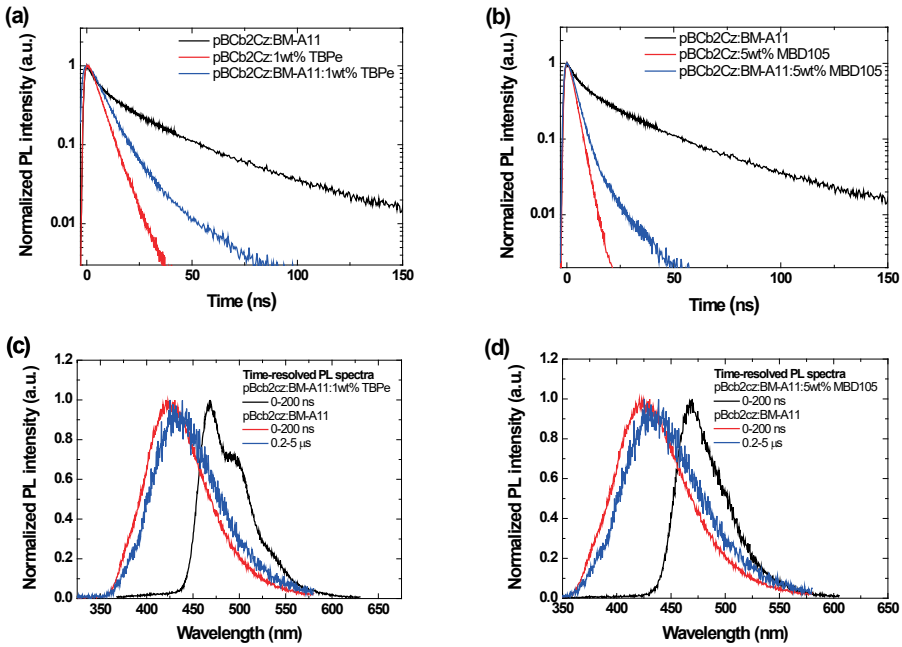

Figure 4.3 Comparison of transient PL data between fluorescent emitters doped in pBCb2Cz:BM-A11 exciplex and neat pBCb2Cz. (a) TBPe (b) MBD105 (c) Time-resolved PL spectra of pBCb2Cz:BM-A11 exciplex film and 1wt% TBPe doped in pBCb2Cz:BM-A11 exciplex film (d) Time-resolved PL spectra of pBCb2Cz:BM-A11 exciplex film and 5wt% MBD105 doped in pBCb2Cz:BM-A11 exciplex film.

To identify the effect of the fluorescent dopant, an OLED was fabricated based on pBCb2Cz:BM-A11 exciplex co-host and TBPe, MBD105 as emitters. The schematic diagram of the device structure and the energy levels of the consisting layers are shown in Figure 4.4a. The device structure of OLEDs was same as follows but only type and concentration of blue fluorescent dopant were different; ITO (70 nm) / 10wt% MoO_3 doped TAPC (35 nm) / TAPC (20 nm) / pBCb2Cz (5 nm) / pBCb2Cz:BM-A11:1wt% TBPe or pBCb2Cz:BM-A11:5wt% MBD105 (30 nm) / BM-A11 (5nm) / CN-T2T (35nm) / LiF (1 nm) / Al (100 nm). 1,1-Bis[(di-4- tolylamino)phenyl]cyclohexane (TAPC) was selected as hole-transport material (HTM) in OLED devices. It's high ionization potential (IP=5.6V) and hole mobility shows good hole injection and transport properties widely used.[86,87]

The fabricated device shows EL emission peak at 464nm indicating efficient Förster energy transfer to TBPe and MBD105. (Figure 4.4b) The current density-voltage-luminance (*J-V-L*) characteristics of the fluorescent OLEDs at room temperature are shown in Figure 4.4c. It shows the turn-on voltage of 3.3V, 3.0V, 3.3V each. The EQEs and luminance of the devices are displayed in Figure 4.4d. The maximum efficiency of the exciplex OLEDs was 0.53% with a deep blue

emission, TBPe-doped fluorescent OLEDs was 5.22% with blue emission and MBD105-doped fluorescent OLEDs was 4.81% with deep blue emission. Detailed characteristics of the device are summarized in table 4.2.

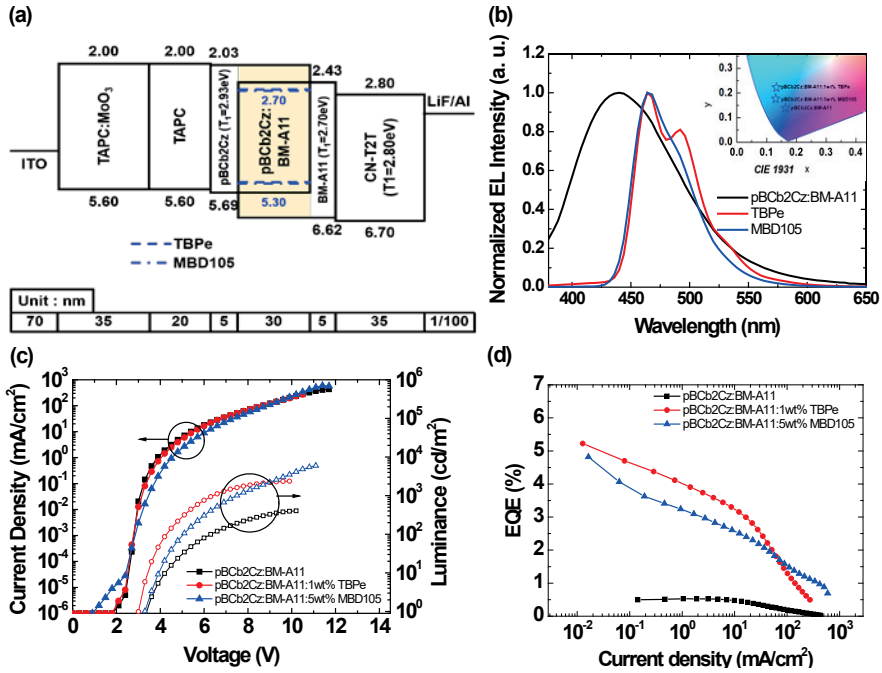

Figure 4.4 (a) Schematic diagram of the blue fluorescent device structure and energy levels of the consisting layers of pBCb2Cz:BM-A11 exciplex forming co-host based OLED and TBPe, MBD105 fluorescent OLEDs (b) Electroluminescence (EL) spectra at 1,000 cd m^{-2}. (c) Current density-voltage-luminance (*J-V-L*) characteristics (d) External quantum efficiencies (EQEs) of OLEDs as a function of luminance.

- 10wt% MoO_3 was doped to TAPC for better charge injection.
- Every substrate was annealed at 250 °C for 30min before evaporation.
- HOMO levels of TAPC and TCTA: CV measurement
- LUMO levels of TAPC and TCTA: HOMO levels + the optical gap
- LUMO levels of CN-T2T: CV measurement
- HOMO levels of CN-T2T: LUMO levels + the optical gap
- Energy levels of EML: transporting energy

Table 4.2 Device characteristics of the exciplex-based OLEDs and fluorescent OLEDs

Device	V_{on}	EQE (%)		PE (lm W^{-1})		CIE (x,y) at 1000 cd m^{-2}
		Max.	1000 cd m^{-2}	Max.	1000 cd m^{-2}	
pBCb2Cz:BM-A11	3.3	0.53	-	0.49	-	(0.16, 0.13)
pBCb2Cz:BM-A11+1wt% TBPe	3.0	5.22	2.81	8.22	2.16	(0.13, 0.22)
pBCb2Cz:BM-A11+5 wt% MBD105	3.3	4.81	2.07	5.96	1.15	(0.13, 0.17)

To confirm how much amount of sensitizing effect occurred in fabricated device, simulation was performed using Luxol software, which allows the fabrication of virtual devices and extraction of device properties. Comparison of the EQE value between simulated achieved one and experimentally achieved one. EQE values obtained through simulation (line-plot) depending on ETL thickness and experimentally achieved maximum EQE data (circle-dot-scatter) are shown in figure 4.5a. The experimental value was about 0.08, 0.4 values as high for TBPe, MBD105 fluorescent OLEDs when comparing the experimentally obtained value with that obtained from the simulation.

Figure 4.5b shows the decay of the EL intensity of the OLEDs as a function of operating time under constant current at an initial luminance (L_0) of 400 cd m^{-2}. The LT_{50} lifetime of the blue fluorescent OLEDs was 0.44 h, 2.71 h at 400 cd m^{-2} in TBPe, MBD105 doped with pBCb2Cz:BM-A11 exciplex system. This result is about 5 times better than TBPe doped with mCBP:TSPO1 co-host system[14] I assumed this prolonged lifetime comes from delayed fluorescence of exciplex compared with non-exciplex forming mCBP:TSPO1 co-host.

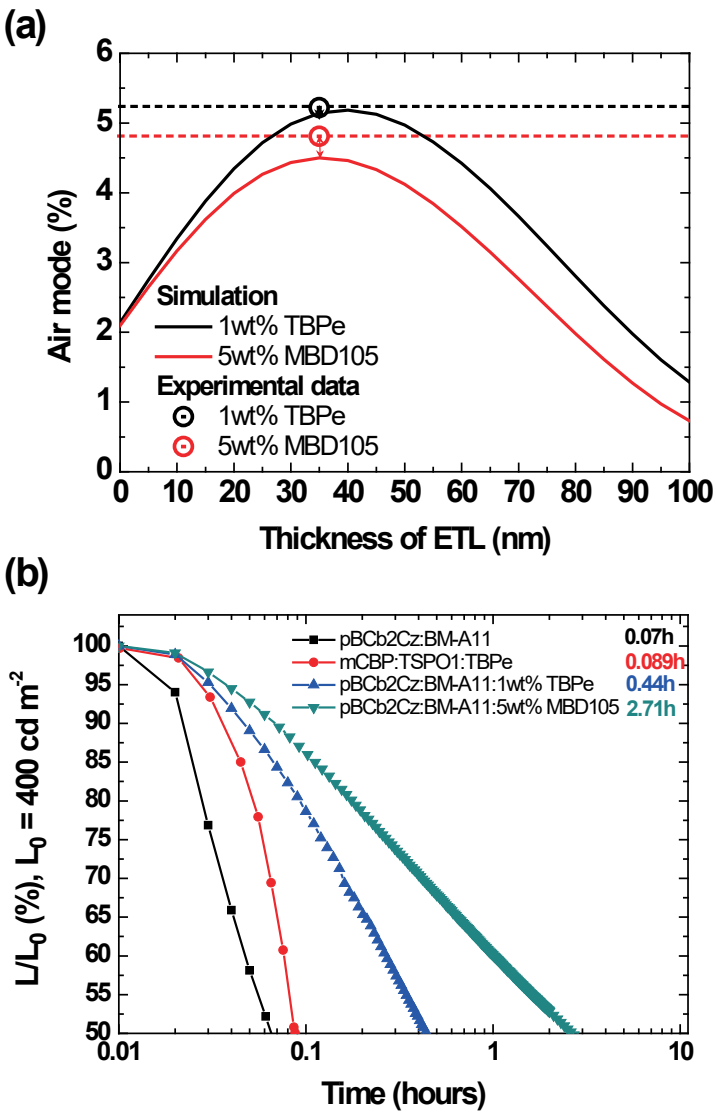

Figure 4.5 (a) Comparison of maximum EQE values obtained through simulation (line-plot) and experimental (circle-dot-scatter) (b) Operational lifetime of fluorescent OLEDs at an initial luminance (L_0) of 400 cd m^{-2}

4.4 Conclusion

I designed a novel deep blue-exciplex forming co-host. Then, fabricated blue fluorescent OLEDs with fixed EL peak wavelength (464nm). The fluorescent OLEDs based on pBCb2Cz:BM-A11 exciplex shows a maximum EQE of 5.22% (TBPe), 4.81% (MBD105). The LT_{50} lifetime of the blue fluorescent OLEDs was 0.44 h (TBPe), 2.71 h (MBD105) at 400 cd m^{-2}. Comparison with previously reported conventional blue fluorescent OLEDs, this result is about 5 times better than TBPe doped with mCBP:TSPO1 co-host.[14]

Chapter 5. Summary and Conclusion

OLEDs are addressed in the new field of flat-panel display and solid-state lighting due to their various advantages in a wide fields. Since there are many advantages and application are expected, active researches are underway after it discovered in 1987. However, still, blue OLEDs are recognized as scientific challenges in high efficiency and operational stability compare with other emission colors due to its large bandgap and selection of stable materials. Until now, studies of blue exciplexes are rarely reported for these reasons. If an exciplex showing blue emission is found, a wide range of applications may be possible in OLEDs.

For this reason, this thesis focusing on greenish-blue to blue region of exciplex forming co-host based OLEDs which can efficiently harvest triplet excitons using exciplex co-host and using conventional dyes for better color coordinate and operational stability of the device.

In **Chapter 2**, the novel greenish-blue exciplex forming co-host with better-delayed component constants and delayed emission portions were reported. For optimizing device structure, a 5nm pure donor layer was inserted between HTM and EML, which maximum EQE showed

about 1.4 times higher than the device without a pure donor layer. This maximum EQE value indicates that at least 63% and at most 72% of the radiative singlet excitons (η_s) are involved in the luminescence when comparing the simulation results with experimental values. Also, EL spectra red-shifted occur while applying voltage increment in H2:PO-T2T exciplex-based OLEDs, and it defined as its own characteristics.

Using exciplex with better-delayed fluorescence as reported in Chapter 2, I tried to focus on device stability in **Chapter 3**. By using conventional fluorescent dopant with better PLQY, the yellow fluorescent OLEDs based on exciplex co-host showed maximum EQE 7.2%, with extended lifetime (60 h) at 1,000 cd m^{-2} until initial luminance decreases to LT_{50}. Compared with previously reported results in the same condition (only exciplex system difference), these results are about 8.5 times higher than TCTA:B4PYMPM:2wt% TBRb.

In **Chapter 4**, I found novel blue exciplex forming co-host with triplet energy above 2.70 eV for consisting materials. For an effective triplet harvesting process, I use exciplex forming co-host as a sensitizer expecting sensitizing effect with fluorescent emitters. Also, for the purpose of better color coordinate with device stability, blue fluorescent

dopants were doped with a blue exciplex system. As a result, the blue fluorescent OLEDs based on exciplex forming co-host showed EQE of 5.22, 4.81%. These maximum EQE values were achieved by experiment.

I believe that still more research should need for a better future of OLEDs. Organic materials with good opto-electronic properties such as stability, suitable energy level, more radiative excitons, reduced non-radiative excitons, I believe someday highly efficient OLEDs with a long operational lifetime will be invent.

Bibliography

[1] C. W. Tang, S. A. VanSlyke, *Appl. Phys. Lett*. **1987**, *51*, 913.

[2] S.-Y. Kim, W.-I. Jeong, C. Mayr, Y.-S. Park, K.-H. Kim, J.-H. Lee, C.-K. Moon, W. Brütting, J.-J. Kim, *Adv. Funct. Mater.* **2013**, *23*, 3896.

[3] C.-K. Moon, K.-H. Kim, J.-W. Lee, J.-J. Kim, *Chem. Mater.* **2015**, *27*, 2767.

[4] Y. Kawamura, J. Brooks, J. J. Brown, H. Sasabe, C. Adachi, *Phys. Rev. Lett.***2006**, *96*, 017404.

[5] M. A. Baldo, D. F. O'Brien, Y. You, A. Shoustikov, S. Sibley, M. E. Thompson, S. R. Forrest, *Nature* **1998**, *395*, 151.

[6] H. Uoyama, K. Goushi, K. Shizu, H. Nomura, C. Adachi, *Nature* **2012**, *492*, 234.

[7] H. Nakanotani, K. Masui, J. Nishide, T. Shibata, C. Adachi, *Sci. Rep*. **2013**, *3*, 2127.

[8] M. A. Baldo, S. Lamansky, P. E. Burrows, M. E. Thompson, S. R. Forrest, *Appl. Phys. Lett.* **1999**, *75*, 4.

[9] M. A. Baldo, M. E. Thompson, S. R. Forrest, *Nature*, **2000**, *403*, 750.

[10] H. Nakanotani, T. Higuchi, T. Furukawa, K. Masui, K. Morimoto, M. Numata, H. Tanaka, Y. Sagara, T. Yasuda, C. Adachi, *Nat. Commun*. **2014**, *5*, 4016.

[11] D. Zhang, L. Duan, C. Li, Y. Li, H. Li, D. Zhang, Y. Qiu, *Adv. Mater*. **2014**, *26*, 5050.

[12] H.-G. Kim, K.-H. Kim, C.-K. Moon, J.-J. Kim, *Adv. Opt. Mater*. **2017**, *5*, 1600749.

[13] H.-G. Kim, K.-H. Kim, J.-J. Kim, *Adv. Mater*. **2017**, *29*, 1702159.

[14] H.-G. Kim, H. Shin, Y. H. Ha, R. Kim, S. K. Kwon, Y. H. Kim, J.-J. Kim, *ACS Appl. Mater. Interfaces,* **2018**, *11*, 26.

[15] M. Segal, M. Singh, K. Rivoire, S. Difley, T. Van Voorhis, M. A. Baldo, *Nat. Mater.* **2007**, *6*, 374.

[16] D. Y. Kondakov, *J. Soc. Inf. Display* **2009**, *17*, 137.

[17] C.-J. Chiang, A. Kimyonok, M. K. Etherington, G. C. Griffiths, V. Jankus, F. Turksoy, A. P. Monkman, *Adv. Funct. Mater*. **2013**, *23*, 739.

[18] S. M. King, M. Cass, M. Pintani, C. Coward, F. B. Dias, A. P. Monkman, M. Roberts, *J. Appl. Phys*. **2011**, *109*, 074502.

[19] V. Jankus, C. J. Chiang, F. Dias, A. P. Monkman, *Adv. Mater*. **2013**, *25*, 1455.

[20] D. Graves, V. Jankus, F. B. Dias, A. P. Monkman, *Adv. Funct. Mater*. **2014**, *24*, 2343.

[21] B. C. Krummacher, S. Nowy, J. Frischeisen, M. Klein, W. Brütting, *Org. Electron*. **2008**, *10*, 478.

[22] S. Nowy, B. C. Krummacher, J. Frischeisen, N. A. Reinke, W. Brütting, *J. Appl. Phys.* **2008**, *104*, 123109.

[23] H. Becker, S. E. Burns, R. H. Friend, *Phys. Rev. B* **1997**, *56*, 1893.

[24] J. A. E. Wasey, A. Safonov, I. D. W. Samuel, W. L. Barnes, *Phys. Rev. B,* **2001**, *64*, 205201.

[25] J. A. E. Wasey, W. L. Barnes, *J. Mod. Opt.* **2000**, *47*, 725.

[26] J.-S. Kim, P. K. Ho, N. C. Greenham, R. H. Friend, *J. Appl. Phys*. **2000**, *88*, 1073.

[27] J. Frischeisen, D. Yokoyama, A. Endo, C. Adachi, W. Brütting, *Org. Electron.* **2011**, *12*, 809.

[28] K.-H. Kim, S. Lee, C.-K. Moon, S.-Y. Kim, Y.-S. Park, J.-H. Lee, J. W. Lee, J.-S. Huh, Y. You, J.-J. Kim, *Nat. Commun.* **2014**, *5*, 4769.

[29] H. Shin, S. Lee, K.-H. Kim, C.-K. Moon, S.-J. Yoo, J.-H. Lee, J.-J. Kim, *Adv. Mater.* **2014**, *26*, 4730.

[30] T.-A. Lin, T. Chatterjee, W.-L. Tsai, W.-K. Lee, M.-J. Wu, M. Jiao, K.-C. Pan, C.-L. Yi, C.-L. Chung, K.-T. Wong, C.-C. Wu, *Adv. Mater*. **2016**, *28*, 6976.

[31] K.-H. Kim, E.-S. Ahn, J.-S. Huh, Y.-H. Kim, J.-J. Kim, *Chem. Mater.* **2016**, *28*, 7505.

[32] M. Liu, R. Komatsu, X. Cai, K. Hotta, S. Sato, K. Liu, D. Chen, Y. Kato, H. Sasabe, S. Ohisa, Y. Suzuri, D. Yokoyama, S. J. Su, J. Kido, *Chem. Mater.* **2017**, *29*, 8630.

[33] P. Rajamalli, N. Senthilkumar, P.-Y. Huang, C.-C. Ren-Wu, H.-W. Lin, C.-H. Cheng, *J. Am. Chem. Soc.* **2017**, *139*, 10948.

[34] J. Frischeisen, D. Yokoyama, C. Adachi, W. Brütting, *Appl. Phys. Lett.* **2010**, *96*, 29.

[35] K.-H. Kim, C.-K. Moon, J.-H. Lee, S.-Y. Kim, J.-J. Kim, *Adv. Mater*. **2014**, *26*, 3844.

[36] J. W. Sun, J. Y. Baek, K.-H. Kim, J.-S. Huh, S.-K. Kwon, Y.-H. Kim, J.-J. Kim, *J. Mater. Chem. C* **2017**, *5*, 1027.

[37] K.-H. Kim, J.-J. Kim, *Adv. Mater.* **2018**, *30*, 1705600.

[38] S.-Y. Byeon, J. Kim, D.-R. Lee, S.-H. Han, S. R. Forrest, J.-Y. Lee, *Adv. Opt. Mater.* **2018**, *6*, 1701340.

[39] C.-S. Oh, C.-K. Moon, J. M. Choi, J. S. Huh, J.-J. Kim, J.-Y. Lee, *Org. Electron.* **2017**, *42*, 337.

[40] T. Matsushima, F. Bencheikh, T. Komino, M. R. Leyden, A. S. Sandanayaka, C. Qin, C. Adachi, *Nature*, **2019**, *572*, 502.

[41] X.-K. Liu, Z. Chen, C. J. Zheng, M. Chen, W. Liu, X. H. Zhang, C. S. Lee, *Adv. Mater.* **2015**, *27*, 2025.

[42] G. J. Kavarnos, N. J. Turro, *Chem. Rev.* **1986**, *86*, 401.

[43] H.-B. Kim, D. Kim, J.-J. Kim, *Highly Efficient OLEDs: Materials Based on Thermally Activated Delayed Fluorescence*; Wiley-VCH: Weinheim, Germany, **2018**, 331.

[44] N. J. Turo, Modern Molecular Chemistry; University Science Books: Sausalito, California, USA, **1991**.

[45] K. Goushi, C. Adachi, *Appl. Phys. Lett.* **2012**, *101*, 23306.

[46] K. Goushi, K. Yoshida, K. Sato, C. Adachi, *Nat. Photonics* **2012**, *6*, 253.

[47] Y.-S. Park, K.-H. Kim, J.-J. Kim, *Appl. Phys. Lett.* **2013**, *102*, 153306.

[48] N. Tamoto, C. Adachi, K. Nagai, *Chem. Mater.* **1997**, *9*, 1077.

[49] C. Giebeler, H. Antoniadis, D. D. C. Bradley, Y. Shirota, *J. Appl. Phys.* **1999**, *85*, 608.

[50] H. Antoniadis, M. Inbasekaran, E. P. Woo, *Appl. Phys. Lett.* **1998**, *73*, 3055.

[51] L. C. Palilis, A. J. Makinen, M. Uchida, Z. H. Kafafi, *Appl. Phys. Lett.* **2003**, *82*, 2209.

[52] K.-H. Kim, S.-J. Yoo, J.-J. Kim, *Chem. Mater.* **2016**, *28*, 1936.

[53] J. Li, H. Nomura, H. Miyazaki, C. Adachi, *Chem. Commun.* **2014**, *50*, 6174.

[54] W. Liu, J.-X. Chen, C.-J. Zheng, K. Wang, D.-Y. Chen, F. Li, Y.-P. Dong, C.-S. Lee, X.-M. Ou, X.-H. Zhang, *Adv. Funct. Mater.* **2016**, *26*, 2002.

[55] Y. T. Hung, Z. Y. Chen, W. Y. Hung, D. G. Chen, K.-T. Wong, *ACS Appl. Mater. Interfaces*, **2018**, *10*, 34435.

[56] M. Chapran, R. Lytvyn, C. Begel, G. Wiosna-Salyga, J. Ulanski, M. Vasylieva, D. Volyniuk, P. Data, J. V. Grazulevicius, *Dye. Pigment.* **2019**, *162*, 872.

[57] M. Chapran, P. Pander, M. Vasylieva, G. Wisona-Salyga, J. Ulanski, F. B. Dias, P. Data, *ACS Appl. Mater. Interfaces,* **2019**, *11*, 13460.

[58] S.-K. Jeon, H.-J. Jang, J.-Y. Lee, *Adv. Opt. Mater.* **2019**, *7*, 1801462.

[59] B. Li, L. Gan, X. Cai, X.-L. Li, Z. Wang, K. Gao, D. Chen, Y. Cao, S.-J. Su, *Adv. Mater. Interfaces*, **2018**, *5*, 1800025.

[60] B. Zhao, T. Zhang, B. Chu, W. Li, Z. Su, Y. Luo, R. Li, X. Yan, F. Jin, Y. Gao, H. Wu, *Org. Electron*. **2015**, *17*, 15.

[61] J.-H. Lee, S.-H. Cheng, S.-J. Yoo, H. Shin, J.-H. Chang, C.-I. Wu, K.-T. Wong, J.-J. Kim, *Adv. Funct. Mater.* **2015**, *25*, 361.

[62] H. Lim, H. Shin, K.-H. Kim, S.-J. Yoo, J.-S. Huh and J.-J. Kim, *ACS Appl. Mater. Interfaces*, **2017**, *9*, 37883.

[63] C. J. Shih, C. C. Lee, T. H. Yeh, S. Biring, K. K. Kesavan, N. R. A. Amin, M. H. Chen, W. C. Tang, S. W. Liu and K.-T. Wong, *ACS Appl. Mater. Interfaces*, **2018**, *10*, 24090.

[64] Q. S. Tian, L. Zhang, Y. Hu, S. Yuan, Q. Wang and L. S. Liao, *ACS Appl. Mater. Interfaces*, **2018**, *10*, 39116.

[65] T. Xu, J. G. Zhou, C. C. Huang, L. Zhang, M. K. Fung, I. Murtaza, H. Meng and L. S. Liao, *ACS Appl. Mater. Interfaces*, **2017**, *9*, 10955.

[66] S.-J. Su, H. Sasabe, T. Takeda, J. Kido, *Chem. Mater*. **2008**, *20*, 1691.

[67] W. Y. Hung, P. Y. Chiang, S. W. Lin, W. C. Tang, Y. T. Chen, S. H. Liu, P. T. Chou, Y. T. Hung, K.-T. Wong, *ACS Appl. Mater. Interfaces* **2016**, *8*, 4811.

[68] T. Zhang, B. Zhao, B. Chu, W. Li, Z. Su, X. Yan, C. Liu, H. Wu, Y. Gao, F. Jin, F. Hou, *Sci. Rep.* **2015**, *5*, 10234.

[69] B. Zhao, T. Zhang, B. Chu, W. Li, Z. Su, H. Wu, X. Yan, F. Jin, Y. Gao, C. Liu, *Sci. Rep.* **2015**, *5*, 10697.

[70] K.-H. Kim, C.-K. Moon, J.-W. Sun, B. Sim, J.-J. Kim, *Adv. Opt. Mater.* **2015**, *3*, 895.

[71] J. J. Tomes, C. E. Finlayson, *Eur. J. Phys.* **2016**, *37*, 055501.

[72] B. C. Krummacher, S. Nowy, J. Frischeisen, M. Klein, W. Brütting, *Org. Electron.* **2009**, *10*, 478.

[73] S. Nowy, B. C. Krummacher, J. Frischeisen, N. A. Reinke, W. Brütting, *J. Appl. Phys.* **2008**, *104*, 123109.

[74] D. Yokoyama, *J. Mater. Chem.* **2011**, *21*, 19187.

[75] D. Yokoyama, A. Sakaguchi, M. Suzuki, C. Adachi, *Org. Electron*. **2009**, *10*, 127.

[76] G. Tian, W. Liang, Y. Chen, N. Xiang, Q. Dong, J. Huang, J.-H. Su, *Dye. Pigment.* **2016**, *126*, 296.

[77] X.-K. Liu, Z. Chen, C.-J. Zheng, C.-L. Liu, C.-S. Lee, F. Li, X.-M. Ou, X.-H. Zhang, *Adv. Mater.* **2015**, *27*, 2378.

[78] W. Y. Hung, G. C. Fang, S. W. Lin, S. H. Cheng, K. T. Wong, T. Y. Kuo, P. T. Chou, *Sci. Rep.* **2014**, *4*, 5161.

[79] S. Yin, Z. Shuai, Y. Wang, *J. Chem. Inf. Comput. Sci.* **2003**, *43*, 970.

[80] X.-L. Li, G. Xie, M. Liu, D. Chen, X. Cai, J. Peng, Y. Cao, S.-J. Su, *Adv. Mater*. **2016** *28*, 4614.

[81] B. Zhao, Y. Miao, Z. Wang, W. Chen, K. Wang, H. Wang, Y. Hao, B. Xu, W. Li, *Org. Electron*. **2016**, *37*, 1.

[82] X. Wang, R. Wang, D. Zhou, J. Yu, *Syn. Met.* **2016**, *214*, 50.

[83] J.-W. Sun, J.-H. Lee, C.-K. Moon, K.-H. Kim, H. Shin, J.-J. Kim, *Adv. Mater.* **2014**, *26*, 5684.

[84] J.-W. Sun, K.-H. Kim, C.-K. Moon, J.-H. Lee, J.-J. Kim, *ACS Appl. Mater. Interfaces,* **2016**, *8*, 9806.

[85] Y.-S. Wu, T.-H. Liu, H.-H. Chen, C. H. Chen, *Thin Solid Films* **2006**, *496*, 626.

[86] T. Lin, Q. Song, Z. Liu, B. Chu, W. Li, Y. Luo, C. S. Lee, Z. Su, Y.

Li, *Syn. Met.* **2017**, *234*, 95.

[87] B. Sun, W. Hong, C. Guo, S. Sutty, H. Aziz, Y. Li, *Org. Electron*. **2016**, *37*, 190.

[88] H. Jung, S. Kang, H. Lee, Y.-J. Yu, J. H. Jeong, J. Song, Y. Jeon, J. Park, *ACS Appl. Mater. Interfaces* **2018**, *10*, 30022.

[89] A. L. Von Ruden, L. Cosimbescu, E. Polikarpov, P. K. Koech, J. S. Swensen, L. Wang, J. T. Darsell, A. B. Padmaperuma, *Chem. Mater.* **2010**, *22*, 5678.

[90] S. J. Kim, Y. J. Kim, Y. H. Son, J. A. Hur, H. A. Um, J. Shin, T. W. Lee, M. J. Cho, J. K. Kim, S. Joo, J. H. Yang, G. S. Chae, K. Choi, J. H. Kwon, D. H. Choi, *Chem. Commun*. **2013**, *49*, 6788.

[91] F. C. De Lucia Jr., T. L. Gustafson, D. Wang, A. J. Epstein, *Phys. Rev. B* **2002**, *65*, 235204.

[92] J. Yang, K. C. Gordon, *Chem. Phys. Lett.* **2003**, *375*, 649.

[93] X. Jiang, R. A. Register, K. A. Killeen, M. E. Thompson, F. Pschenitzka, T. R. Hebner, J. C. Sturm, *J. Appl. Phys*. **2002**, *91*, 6717.

[94] W.-Y. Hung, T. C. Wang, P. Y. Chiang, B. J. Peng, K. T. Wong, *ACS Appl. Mater. Interfaces* **2017**, *9*, 7355.

[95] T.-C. Lin, M. Sarma, Y. T. Chen, S. H. Liu, K. T. Lin, P. Y. Chiang, W.-T. Chuang, Y.-C. Liu, H.-F. Hsu, W.-Y. Hung, W. C. Tang, K.-T. Wong, P.-T. Chou, *Nat. Commun*. **2018**, *9*, 3111.

[96] Z. Chen, X.-K. Liu, C.-J. Zheng, J. Ye, C.-L. Lin, F. Li, X.-M. Ou, C.-S. Lee, X.-H. Zhang, *Chem. Mater.* **2015**, *27*, 5206.

[97] W. Song, K.-S. Yook, *J. Ind. Eng. Chem.* **2018**, *61*, 445.

[98] A. R. Brown, D. D. C. Bradley, J. H. Burroughes, R. H. Friend, N. C. Greenham, P. L. Burn, A. B. Holmes, A. Kraft, *Appl. Phys. Lett.* **1992**, *61*, 2793.

[99] C. Adachi, R. C. Kwong, P. Djurovich, V. Adamovich, M. A. Baldo,

M. E. Thompson, S. R. Forrest, *Appl. Phys. Lett.* **2001**, *79*, 2082.

[100] T. Tsuboi, H. Murayama, S.-J. Yeh, C.-T. Chen, *Opt. Mater.* **2007**, *29*, 1299.

[101] Q. S. Zhang, D. Tsang, H. Kuwabara, Y. Hatae, B. Li, T. Takahashi, S. Y. Lee, T. Yasuda, C. Adachi, *Adv. Mater*. **2015**, *27*, 2096.

[102] W. Song, J. Y. Lee, *IMID Digest* **2015**, 56.

[103] D. D. Zhang, X. Z. Song, M. H. Cai, L. Duan, *Adv. Mater.* **2018**, 30, 1705250.

[104] H. Shin, J.-H. Lee, C.-K. Moon, J.-S. Huh, B. Sim, J.-J. Kim, *Adv. Mater.* **2016**, *28*, 4920.

[105] H. Lim, H. Shin, K.-H. Kim, S.-J. Yoo, J.-S. Huh, J.-S. Kim, J.-J. Kim, *ACS Appl. Mater. Interfaces* **2017**, *9*, 37883.

[106] S.-H. Han, J.-Y. Lee, *J. Mater. Chen. C* **2018**, *6*, 1504.

[107] I.-H. Lee, W. Song, J.-Y. Lee, S.-H. Hwang, *J. Mater. Chem. C* **2015**, *3*, 8834.

[108] W. Song, I. Lee, J. Y. Lee, *Adv. Mater.* **2015**, *27*, 4358.

[109] S.-K. Jeon, H.-J. Park, J.-Y. Lee, *ACS Appl. Mater. Interfaces*, **2018**, *10*, 5700.

초 록

디스플레이란 전자 기기의 출력 신호를 시각 정보로 변화시켜서 화면으로 표시해 주는 영상 장치를 포괄하는 단어이다. 디스플레이 산업은 액정표시장치, 광 발광 다이오드, 유기발광 다이오드, 마이크로 및 대면적 디스플레이에 이르기까지 계속해서 개발이 이루어졌고 현재에도 활발한 연구가 계속되고 있다.

유기 발광 다이오드는 유기물을 사용하여 백라이트 없이도 색과 빛을 발현하는 자체 발광 디스플레이를 의미한다. 유기 발광 다이오드의 작동원리는 다음과 같다. 외부 전압을 가하면 전극으로부터 전자와 정공이 주입되어 만나서 엑시톤을 형성하여 빛 에너지를 방출한다.

유기 발광 다이오드는 백라이트나 색 필터가 필요하지 않아서 부피를 줄일 수 있고 낮은 소비 전력, 빠른 반응 속도, 뛰어난 명암비, 넓은 시야각, 투명성을 띠거나 유연하며 접을 수 있는 디스플레이로의 확장 가능성 등의 장점이 있으며,

때문에 유기 발광 다이오드는 차세대 디스플레이로써 주목받고 있다. 그러나 여전히 유기 발광 다이오드 산업화를 위해 극복해야 할 문제들이 존재한다.

유기 발광 다이오드에서 높은 색 순도, 고효율, 긴 소자 구동 수명을 얻기 위해 계속적으로 연구가 진행되고 있다. 색은 발광체의 고유 특성에 의해 결정되므로, 발광체의 적절한 선정이 가장 중요하며 발광체로써 단일 분자, 이종 분자, 엑시플렉스, 형광 염료, 인광 염료, 열 활성 지연 형광 재료 등 다양한 물질들이 이용되고 있으며 다채로운 색 발현이 가능해졌다. 여러 색을 발현하는 유기 발광 다이오드 중 청색 유기 발광 다이오드의 경우, 엑시플렉스 공동 호스트 물질 선정에 있어서 전자받개의 LUMO 준위와 전자주개의 HOMO 준위 그리고 엑시플렉스 결합 에너지의 차이가 약 2.8eV 이상의 높은 에너지 준위 차이를 만족해야 한다. 또한 높은 삼중항 에너지를 가지며 청색 발광을 보이는 엑시플렉스를 형성하는 공동 호스트 물질들이 별로 없고, 안정성 측면에서 소자 구동 시 높은 구동 전압이 필요하므로 다른 색을 발현하는 유기 발광 다이오드들보다 효율 및 소자

구동 수명이 낮은 편이다. 따라서 청색 유기 발광 다이오드는 일상생활이나 산업에서 사용하기 위해 해결 되어야 할 문제로 계속해서 연구가 진행되어 왔다.

본 논문은 청록색과 청색 엑시플렉스 공동 호스트 기반 유기 발광 다이오드 및 안정한 기존 형광 염료를 사용한 유기 발광 다이오드 분석에 대한 연구 주제를 다루고 있다.

제 2 장은, 높은 항간 교차 x 역 항간 교차 운동 상수를 가지는 청록색 엑시플렉스 기반 유기 발광 다이오드에 대한 내용을 담고 있다. 높은 열적 안정성을 보이는 분자들을 사용하기 때문에 엑시플렉스를 형성할 때도 높은 안정성이 있을 것으로 생각했다. 두 개의 링이 수직방향으로 상호 결합된 분자 기반의 정공 전달물질과 높은 삼중항 준위를 갖는 산화 포스핀이 포함된 전자 전달물질을 이용하여 2.54 eV 의 발광 에너지 준위를 갖는 새로운 엑시플렉스를 설계하였다. 또한, 이 엑시플렉스는 빠른 초기 감쇄 속도 및 지연 발광되는 비율이 높았으며, 이는 효율적인 삼중항 수확이

가능할 것으로 예측되었다. 새롭게 개발된 엑시플렉스 시스템을 활용하여 10.6%의 최대 양자 효율을 얻었다.

소자 구동 안정성은 유기 발광 다이오드에서 중점적으로 해결해야 할 문제 중 하나이다. 제 3 장은, 앞서 보고한 엑시플렉스 시스템을 활용하는 방안으로 노란색 염료를 사용하여 엑시플렉스 감광효과를 기반으로 하는 늘어난 수명 특성을 갖는 형광 소자를 제작하여 보고하였다. 광 물리적 특성에 따라, 엑시플렉스 발광 스펙트럼과 형광 발광체의 흡수 스펙트럼이 많은 부분에서 중첩이 일어남을 확인했고, 엑시플렉스로부터 형광 도펀트로의 에너지 전달 과정이 효율적으로 발생할 가능성을 보임을 예측할 수 있었다. 노란색 형광 소자는 7.2%의 최대 양자 효율을 보였으며, 1000 cd m^{-2} 에서 50%의 휘도 저감까지 60 시간이 소요되는 노란색 형광 유기 발광 다이오드를 구현하였다.

지난 수십 년 동안 유기 발광 다이오드의 효율과 안정성을 높이기 위해, 다양한 물질 설계와 소자 구조 최적화가 진행되었다. 그러나, 전자 받개의 LUMO 준위와

전자 주개의 HOMO 준위 그리고 엑시플렉스 결합 에너지의 차이가 약 2.8eV 이상의 높은 에너지 준위 차이를 만족하는 청색 엑시플렉스에 적합한 재료를 찾거나 개발하기가 어렵기 때문에 여전히 청색 유기 발광 다이오드의 상용화에 어려움이 있었다. 제 4 장에서는, 새로운 진청색 엑시플렉스 유기 발광 다이오드와 청색 형광 유기 발광 다이오드에 관해 다루고 있다. 엑시플렉스 유기 발광 다이오드의 경우 색 좌표 Commission Internationale de L′ Eclairage (CIE $y < 0.13$) 가 진청색 영역에서 나타났다. 위 엑시플렉스 시스템을 응용하기 위해 청색 형광 도펀트를 사용하여 높은 색 순도를 보이는 청색 형광 유기 발광 다이오드를 제작하였다. 그 결과, 엑시플렉스에 의한 효율적인 삼중항 수확이 가능하게 되었고 최대 양자 효율 5.22%, 4.81% 를 갖는 청색 형광 유기발광 다이오드를 제작하였다.

주요어: 형광 유기 발광다이오드, 엑시플렉스, 최대 외부 양자 효율, 기존 형광 발광체, 효율적인 삼중항 수확, 에너지 전달

학 번: 2018-27446

Acknowledgement (감사의 글)

어린시절 ‘네 꿈은 무엇이니?’ 라는 물음에 “제가 가진 능력을 최대한 활용하여 현대사회에 이바지 하고 싶다.” 라고 말하던 아이는, 첫 도전으로 한 분야의 전문가가 되고자 대학원의 문을 두드렸습니다. 두 번의 사계절을 관악에서 보내며 지나온 시간들을 돌아보면, 연구의 입문에서부터 석사 학위 논문을 마무리 하기까지 많은 분들의 도움이 있었기에 가능했다고 생각합니다. 학위 기간 동안 아낌없는 응원을 보내준 분들께 이 본문을 빌려 감사의 말을 드리고자 합니다.

먼저, 학위기간동안 하고싶은 연구를 할 수 있도록 아낌없는 지원을 해주시고 연구자의 시선에서 생각할 수 있도록 지도해주신 김장주 교수님께 감사의 말씀을 드립니다. 기반이 잘 마련된 연구실에서 연구할 수 있었다는 것이 제게는 큰 행운이었습니다.

학기 중이라 매우 바쁘셨음에도 석사 학위 논문 심사의 심사위원이 흔쾌히 되어주신 장지영 교수님, 박수영 교수님께도 다시 한번 감사의 말씀을 드립니다.

연구자의 길을 먼저 그리고 함께 걸어왔던 유기광전자연구실의 선배님들과 동기들에게도 고마움을 전합니다. 연구할 때 행복해 보이는 창기 형, 코딩 스터디를 이끌어준 창헌이 형, 유쾌한 경훈이 형, 열정적인 민수 형, 마음이 넓고 따뜻한 현이 형, 차분한 재민이 형, 조용한 카리스마 현구 형, 친근한 봄이 누나, 궁금한 게 있으면 언제든지 물어보라고 말씀해주신 범수 형, 어떤 상황에서도 의연한 황범이 형, 꼼꼼하고 책임감이 강한 형철이 형과 진석이 형, 성실하고 분위기를 주도하는 윤제 형, 통찰력이 좋은 승제 형, 논리적이고 뛰어난 상황적응력을 가진 재영이 형, 친절하고 겸손한 규훈이 형, 다양한 활동을 좋아하고 의지가 강한 자윤이, 그리고 인생에 있어서 많은 조언을 해주신 김규식 연구교수님과 이장훈 연구 교수님께도 감사의 인사를 드립니다.

공식적으로 제 이야기를 할 기회가 많이 없어, 본문을 통해 몇마디 적어보고 앞으로의 다짐을 하고자 합니다. 재작년 12 월, 어린시절부터 제가 가장 존경해왔던 두 분중 한분이 소천하셨습니다. ‘알은 하나의 세계이다. 태어나려는 자는 하나의 세계를 깨뜨려야 한다.’ 는 데미안의 구절과 유사했던 대학원 생활은 재작년 12 월을 기점으로, 당시에 알을 깨고 마주한 세계는 선과 악이 공존하는 세계가 되었고 그 과정에서 날개 한쪽이 온전치 못한 상태가 되어버린, 날아가는 방법을 잃어버린 나 자신을 발견할 수 있었습니다. 방향성을 잃었을 때, 제자리에 머물기보다 한 발자국씩 전진해 나아가려고 열심히 살아왔고, 현재는 내면적으로 성숙한 나 자신과 마주하게 되었습니다. 아낌없는 응원과 격려를 지속적으로 보내주신 이관행 교수님, 강홍규 박사님, 훌륭하게 AI 프로젝트를 마무리해주신 공득조 박사님을 비롯한, 아버지를 믿고 따라주셨던 GIST 가족구성원 분들께 진심 어린 감사 인사를 아들이 대신 전해 드립니다.

타지에서도 잊지않고 계속 응원을 보내주고 늘 현명하게 비전을 공유해준 기령이를 포함한 나의 벗들도 고맙습니다.

앞으로의 인생에 어떤 챕터가 쓰여질지는 모르지만 정직함을 기본으로 당당하게 제가 진정으로 좋아하는 것을 좇아서 나아가겠습니다. 아버지, 어머니, 그리고 동생과 모든 가족 구성원 분들께 사랑한다는 말 전해드리며 앞으로도 계속해서 정진해 나가겠습니다.

감사합니다.

2020 년 2 월

함 진 현